



Optimization of fused deposition modeling process parameters for dimensional accuracy using I-optimality criterion



Omar Ahmed Mohamed ^{a,*}, Syed Hasan Masood ^a, Jahar Lal Bhowmik ^b

^a Department of Mechanical and Product Design Engineering, Swinburne University of Technology, Hawthorn, Victoria 3122, Australia

^b Department of Statistics, Data Science and Epidemiology, Swinburne University of Technology, Hawthorn, Victoria 3122, Australia

ARTICLE INFO

Article history:

Received 12 March 2015

Received in revised form 2 December 2015

Accepted 14 December 2015

Available online 21 December 2015

Keywords:

Fused deposition modeling (FDM)

I-optimal design

Analysis of variance (ANOVA)

Optimization

Process parameters

Dimensional accuracy

ABSTRACT

Fused deposition modeling (FDM) is one of the widely used additive manufacturing technologies because it has flexibility and ability to build complex parts. The accuracy of parts fabricated by FDM is greatly influenced by various process parameters. FDM process has a complex mechanism in building parts and often poses difficulty in understanding adequately how conflicting FDM parameters will determine part quality and accuracy. Sectors such as medical implant, telecommunication, electronics and aerospace require increasingly higher levels of dimensional accuracy. Thus, traditional methods of ensuring quality do not effectively address global markets and customer's needs. This study proposes an I-optimality criterion for the optimization of FDM process parameters in order to address the limitations of the commonly used traditional designs. This study also aims to develop mathematical models in order to establish nonlinear relationship between process parameters and dimensional accuracy. The results show that I-optimality criterion is very promising technique in FDM process parameter optimization. Confirmation experiments show that the proposed method has great advantages in the aspect of both accuracy and efficiency compared with traditional methods proposed in previous studies.

© 2015 Elsevier Ltd. All rights reserved.

1. Introduction

Fused deposition modeling (FDM), developed by Stratasys, belongs to the additive manufacturing technologies that allow for quick and clean development of prototypes and functional components. In this process, the layers are formed by extrusion of a plastic filament that is unwound from a coil and supplied to the liquefier head to produce a part. The semi-molten filament acts as a plunger to extrude the material via the nozzle [1]. The process behind this principle is that the materials are deposited in a configuration that preferably yields them layer by layer, and are hardened immediately following extrusion from the nozzle

[2]. Further, this process relies on melting and selective deposition of thin filament of thermoplastic polymer in a cross-sectional design to form a layer of the whole part. The material spool used is mounted on the machine, and the FDM head is moved in horizontal X and Y planes so as to produce a layer in a raster movement [3–5]. The build platform moves vertically and shifts to a lower position upon completion of the part.

Additive manufacturing processes, including the FDM process, are required to deliver high-quality parts. The increasing demands on higher quality of fabricated parts by FDM in the modern manufacturing industry such as medical implant, telecommunication, electronics and aerospace require increasingly higher levels of dimensional accuracy. In such applications, maintaining dimensional accuracy with tight tolerances will ensure dimensional stability and repeatability of the manufactured part. The

* Corresponding author. Tel.: +61 469775155.

E-mail address: Omar.Ahmed.Mohamed@outlook.com (O.A. Mohamed).

quality of the final part fabricated by FDM depends greatly on the process parameters selected. Manufactured part by FDM process suffers from dimensional inaccuracy in comparison with other additive manufacturing processes such as SLS because of the variety of conflicting process parameters which affect the dimensional accuracy individually or collectively in interactions of several parameters [3]. This process has a complex mechanism in fabricating parts exhibiting much difficulty in understanding adequately of how parameters involved determine dimensional accuracy. Thus, establishing effective relationship between process parameters and dimensional accuracy and determination of final optimum parameter settings are vital for designers, equipment developers, and production engineers.

This paper is structured as follows: Section 2 reviews the previous research work. Section 3 introduces some useful information behind using computer generated optimal designs including I-optimality criterion. Section 4 presents the research methodology used. Section 5 presents an analysis of the data obtained from the experiment and developed mathematical models. Section 6 discusses the results. Section 7 presents optimization process. Section 8 presents conclusions.

2. Literature review

Some attempts have been made to improve dimensional accuracy of FDM fabricated parts through appropriate adjustments in the process parameters. Sood et al. [6] studied the influence of process parameters on the dimensional accuracy using Taguchi method and artificial neural networks (ANN). They pointed out the optimal process settings are different for each quality criteria, indicating that the optimal process settings cannot be obtained. For this reason, gray relational grade (GRG) was used to transform three responses into one response. The limitation of this work is that the optimum settings are restricted to the experimental values, where, in fact, the optimum settings are not exactly the same as the parameters' values used in experimental matrix. Thus final optimum parameter settings were not obtained using this approach. Nanchariah et al. [7] carried out an experimental investigation on surface quality and dimensional accuracy by employing the Taguchi method and ANOVA technique. However, in this study, optimum settings of the parameters were not addressed. Zhang and Peng [8] investigated the relationship between process parameters and dimensional error and deformation. They reported that optimum process settings for dimensional error and deformation are varied. However, if the goal is to minimize both dimensional error and deformation together, the study could not provide a definite answer in terms of global solution to this problem. Sahu et al. [9] have applied Taguchi method to study the effect of process variables on part accuracy. However, the use of fuzzy inference system (FIS) requires developing rules. Therefore, it needs appropriate expertise knowledge and prior experience.

The above literature review shows that the quality of manufactured part by FDM is greatly influenced by various process parameters fixed at the time of pre-processing of

the part. Although many experimental, theoretical, numerical and optimization studies have been proposed to improve dimensional accuracy for manufactured part in above literature, they have some common weaknesses and disadvantages summarized as follows. First, most of previous researchers have mainly studied dimensional accuracy of part manufactured by ABS; no work has been done of part manufactured by PC-ABS alloy. Second, traditional experimental design such as Taguchi and GRG were used extensively in previous studies to improve dimensional accuracy. However, traditional techniques are difficult to predict and build a functional relationship between process parameters and dimensional accuracy, for example, in traditional experimental techniques; two-factor interactions are confounded (aliased) with other main and higher interaction effects which produce biased estimates of main and interaction effects. This leads to misleading results in cases where many interactions of the factors have a significant influence on dimensional accuracy. Moreover, final optimal global solution cannot be determined because high-order empirical polynomial models cannot be developed by standard designs which is very important when the goal is optimization [3]. Next, there exists much literature, which employs Taguchi method combined with ANN or fuzzy comprehensive evaluation. This is because ANN and FIS do not provide enough information about factors and their interaction effects on the dimensional accuracy if further analyses using Taguchi and GRG have not been done. However, this approach has its disadvantages, as it increases the complexity of the computational process, requires large amount of data and high level of experience for the appropriate engineering judgment to interpret the results. Fourth, none of the literature considers all parameters with all possible levels affecting dimensional accuracy together and their interactions. This is extremely important in order to take advantage of achieving better accuracy and to obtain a functional relationship between parameters and dimensional accuracy. Finally, standard techniques of ensuring quality are not appropriate to solve complex problems and they do not effectively address global markets and customer's needs. This is because there are a large number of conflicting parameters in FDM process, nonlinear relationship, multi-factor interactions and restrictions (constraints) imposed on the levels of the experimental variables [3]; underscoring the need for this study.

In contrast to previous research, this study attempts to address the limitations of previous studies by developing a method that can improve dimensional accuracy efficiently and effectively. This paper proposes, for the first time, a methodology based on computer-generated optimal designs using I-optimality criterion that is efficient and reliable to solve the optimization problem involving large number of FDM parameters and levels with constraints (irregular experimental matrix) [10]. The proposed method provides better accuracy and performance than previous methods in several instances. In this study, a comprehensive relationship between parameters and dimensional accuracy of part fabricated by PC-ABS is established and mathematical models are also developed. This study provides a comprehensive investigation by considering all

critical process parameters with all possible levels, as well as considering a new parameter – the number of contours, which has not been studied previously. This developed and proposed method was then validated in terms of accuracy and precision. The optimum parameter settings obtained by this method will be applied upon real parts, and the results will be analyzed, discussed, and evaluated. The designed experimental procedure is given in Fig. 1.

3. Methodology

3.1. Experimental work

Fig. 2 provides the details of the standard specimen. The dimensions of the specimens were selected according to ASTM D5418/ASTM D7028 specimen [11–13]. The specimen used in this study was modeled in Pro Engineer version 5 and exported as an STL file. The STL file was then imported to the FDM software (Insight version 9.1) to create the tool path and to set all process parameters to all specimens. A total of 60 specimens were manufactured using FDM Fortus 400 machine (shown in Fig. 3). The model material used for the test specimen was PC-ABS blend, working in conjunction with soluble support material. Dimensional accuracy tests were performed using a micrometer with a high accuracy of 0.01 mm. Five readings along the length, width, and thickness were taken per specimen, then the average percentage change (accuracy) was calculated using Eq. (1), and recorded as the output response of each experimentation run.

$$\Delta D = \left| \frac{D_{EXP} - D_{CAD}}{D_{CAD}} \right| \times 100 \quad (1)$$

where ΔD represents the percentage change in dimension (D), D_{EXP} represents the experimental value and D_{CAD} represents the designed value by CAD model.

3.1.1. Tip calibration and measurements

This study considered four layer thicknesses (0.1270, 0.1778, 0.2540 and 0.3302 mm). In order to change the layer thickness, the nozzle (Tip) has to be changed and re-calibrated physically for every change. Since calibration of the FDM process in the XY and Z-directions affects the dimensional accuracy of fabricated parts, it is important to calibrate the XY and Z-directions in order to prevent inadequately calibrating, support tip plugging and inaccuracy of smaller slices. The calibration procedure involves seven steps:

1. Run Auto-Z-Zero routine
2. Run Tip-to-tip calibration routine
3. Build calibration job on empty build plate (see Fig. 4 (b)), and inspect the number closest to the location on the +X, -X, +Y and -Y sides on the calibration built job using high resolution magnifier where the support layer position must be at the center of all the model layers as shown in blue¹ line in Fig. 4(a). If the support layer

position is not at the center of the model layers as shown in blue line in Fig. 4(c and d), then rebuild calibration job and select increment or decrement to input the X and Y offsets adjustment.

4. Check the calibration in the Z-direction by measuring the thickness of the support layer with a caliper having high accuracy of 0.01 mm.
5. Cut the support layer at the center of the leg using Xacto knife. The cut should be in perpendicular direction to the leg.
6. Inspect the cross-section from the cut support layer box using high resolution magnifier. The cross-section must be in rectangular shape. Otherwise re-build calibration job with increasing the calibration by 0.0254–0.0508 mm until getting a rectangular cross-section. Fig. 5 shows acceptable and not acceptable cross sections.
7. Measure the slice height of the rectangular. If the measured value of slice height is within ± 0.01 mm of the model tip slice height, then no adjustment is needed. Otherwise repeat steps 1–6 until the measured value falls within ± 0.01 mm [14].

3.2. Experimental design

3.2.1. The process parameters selected and their levels

The quality of a part manufactured by FDM primarily depends on the process parameters selected. In this study, process parameters included for investigation, are as follows: layer thickness (A); air gap (B); raster angle (C); build orientation (D); and road width (E). This study also included another critical FDM parameter – the number of contours (F), which has not been studied previously on different quality characteristics. The latter seems to be an important factor for the improvement of mechanical properties; however, its effect on dimensional accuracy is still unknown. Table 1 shows the six selected process parameters and their levels. Other FDM parameters are kept at their fixed level and are shown in Table 2. The levels of these control parameters are selected based on the literature review, experience, their significance, and relevance according to the preliminary pilot investigations, and the permissible low and high levels recommended by the equipment manufacturer. It is desirable to have four or five minimum levels of process parameters to reflect the true behavior of response parameters. In this case, the layer thickness factor has only four levels because these levels are restricted by the nozzle diameter (Tip size) as there are only four types of Tip sizes for PC-ABS materials. In order to change the level of layer thickness, the nozzle has to be changed and re-calibration physically for every change. However, other factors are flexible and they can be at six levels with some constraints.

The process parameters are shown graphically in Fig. 6 and are defined as follows [1]:

- (a) *Layer thickness* refers to the thickness of the layer processed by the nozzle tip. The layer thickness depends on the material used and tip size, as shown in Fig. 6(c).

¹ For interpretation of color in Fig. 4, the reader is referred to the web version of this article.

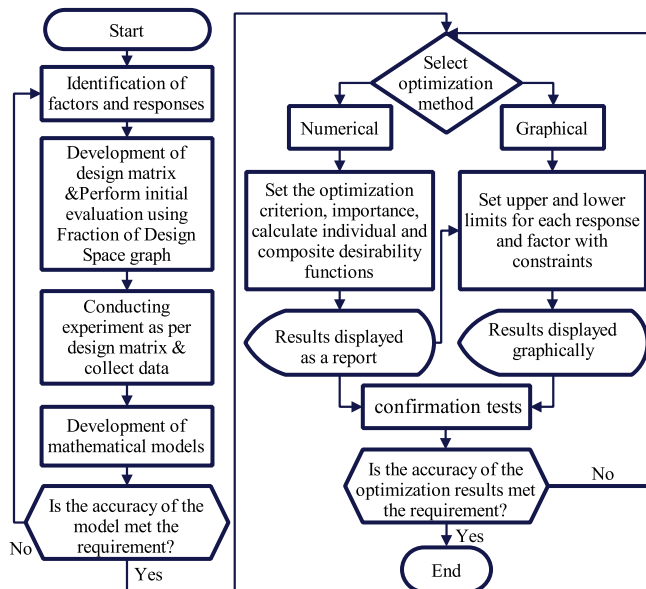


Fig. 1. Flowchart showing methodology applied in this study.

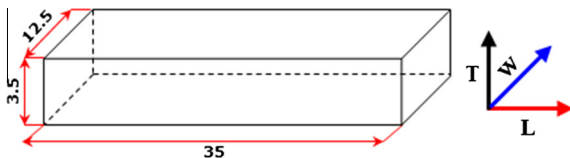


Fig. 2. CAD model of testing specimen (in mm).

- (b) Air gap is the gap between two rasters on the same layer, as shown in Fig. 6(a).
- (c) Raster angle refers to the angle of the raster pattern with respect to the x axis on the bottom part layer, as shown in Fig. 6(a). Specifying the raster angle is very important in parts that have small curves. The raster angles typically allowed are from 0° to 90°.

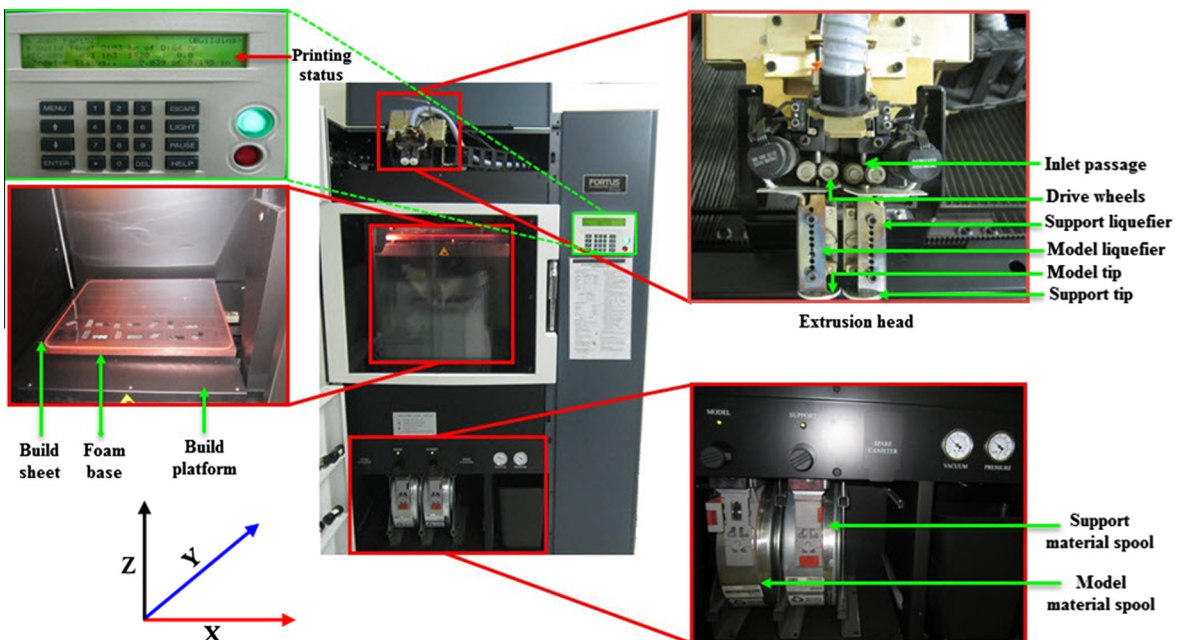


Fig. 3. Details of fused deposition modeling process in Stratasys Fortus 400.

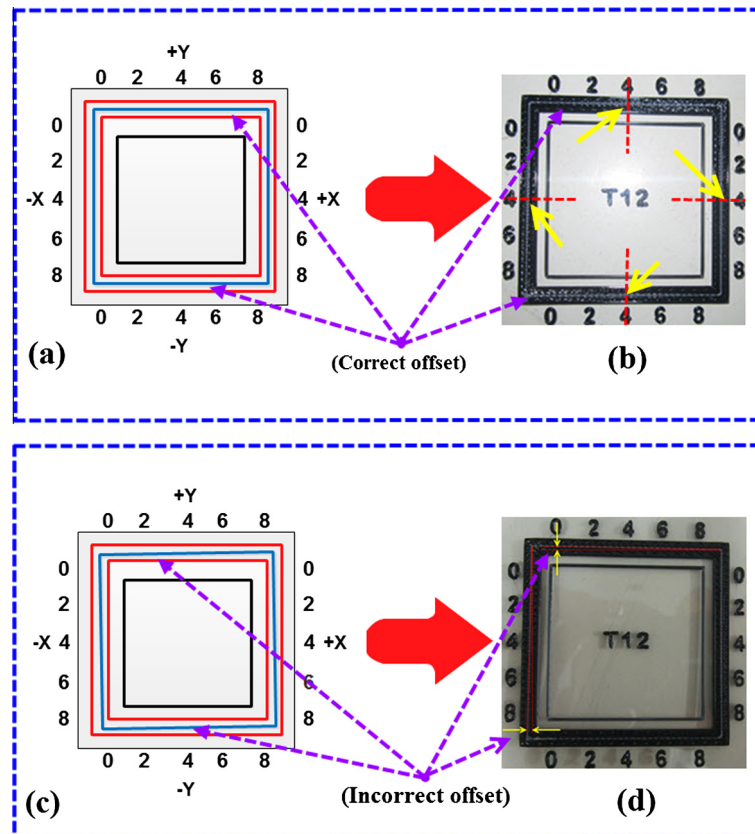


Fig. 4. Support layer position, (a and b) is at the center of all the model layers, and (c and d) is not at the center of all the model layers.

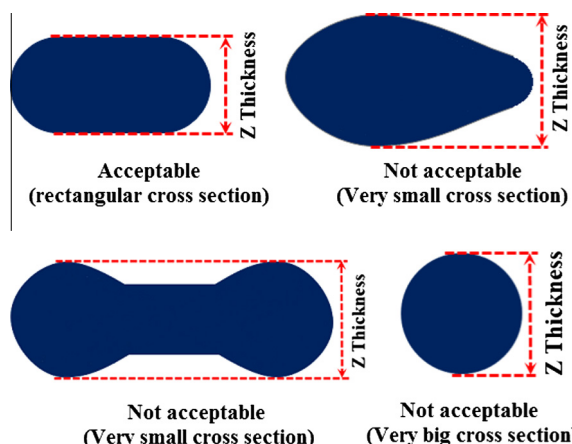


Fig. 5. Acceptable and unacceptable cross sections.

- (d) *Build orientation* refers to the way in which the part is oriented on the build platform with respect to X, Y, Z axes, as shown in Fig. 6(b).
- (e) *Road width* is the width of the material bead used for the rasters, as shown in Fig. 6(a). Larger values of road width will build a part with a stronger interior. Smaller values will require less production time and material.

(f) *Number of contours* is the number of contours built around all outer and inner part curves, as shown in Fig. 6(a). Additional contours may improve perimeter part walls.

3.2.2. Development of design matrix

The pressure from companies to deliver more in terms of quality and productivity improvement has led to the development and use of computer-generated optimal designs. Such an approach helps in generating a design that will satisfy experimental constraints, which occur in the case of optimization of FDM process parameters. Computer-generated optimal designs are appropriate in irregularly shaped experimental regions and in nonstandard models. In most cases, they are generated using point exchange algorithms that select design points from a candidate to optimize a design criterion [15]. There are various statistical designs for satisfying a given criteria: A-optimal design minimizes the trace of the variance-covariance matrix; D-optimal design minimizes the covariance in the parameter estimation; G-optimal design minimizes the maximum of the predicted variance; and I-optimal design reduces the prediction variance across the factor space. Generally, A and D criteria are the most appropriate for first-order models because they are related to parameter estimation, which is important in building factorial designs or screen designs, and where the goal is to find fac-

Table 1

Control factors and their levels.

Symbols	Input factors	Units	Levels					
			1	2	3	4	5	6
A	Layer thickness	mm	0.1270	0.1778	0.2540	0.3302	–	–
B	Air gap	mm	0	0.1	0.2	0.3	0.4	0.5
C	Raster angle	degree	0	15	30	45	60	90
D	Build orientation	degree	0	30	45	60	75	90
E	Road width	mm	0.4572	0.4814	0.5056	0.5298	0.5540	0.5782
F	Number of contours	–	1	3	5	7	8	10

Table 2

Fixed factors and their levels.

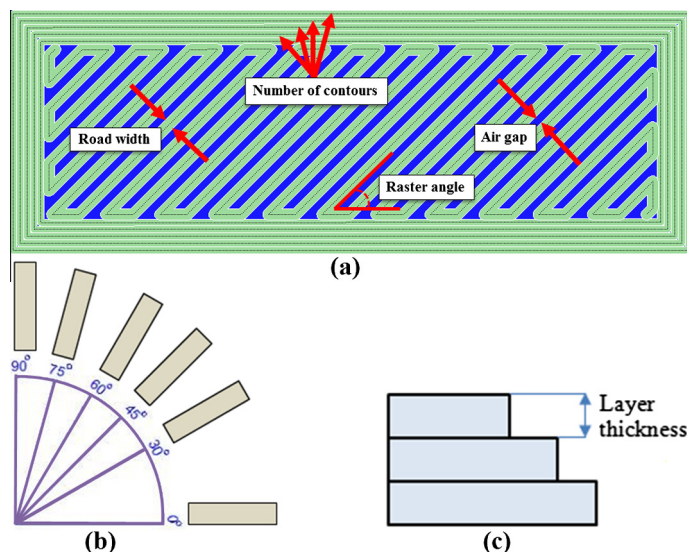
Factor	Level	Unit
Contour to contour air gap	0.0000	mm
Contour to raster air gap	0.0000	mm
Contour width	0.4572	mm
Part X Y shrink factor	1.0075	–
Part Z shrink factor	1.0070	–
Part interior style	Solid	–
Visible surface style	Normal	–

tors important to the process. However, G and I criteria are used for second-order designs, which are very important in optimization. The general approach used in designing experiments in these situations will first involve selecting a region of interest for the experiment, and then narrowing down a set of candidate runs from the initial considerations. Finally, a set of points from this candidate list is selected to be used in the design [10].

Optimal designs refer to a set of experimental designs that are projected to give optimal results with respect to a particular statistical dimension. The optimal statistical dimensions are dependent on the design of the model, and the assessment of such optimality is carried out with respect to the given statistical criteria related to the

variance covariance matrix of the estimators [16]. The I-optimality (also known as IV-, Q-, and V-optimality) used in this instance serves the purpose of minimizing the integrated prediction variance over the region of interest [17]. The I-optimality criterion is a novel technique recommended to build response surface designs when the goal is to optimize the factor settings and a process requiring greater precision in the estimation. The less the prediction variance means, the more the accuracy is achieved. In addition, the I-optimality criterion can add constraints to the design space, for instance, by excluding a specific area where responses cannot be measured. Furthermore, I-optimality criterion can add restrictions to the factor settings, where, in some cases, the final optimal settings cannot be used in the machine or in practical applications, for example, as in our case study with the FDM parameters of layer thickness and number of contours.

Study of six parameters using traditional experimental designs such as central composite, full factorial and Taguchi requires 90, 64 and 27 runs, respectively. It can be mentioned that these numbers of runs are only at three levels of each factor (regular designs) without considering replication criteria and extra design points to improve the precision of the design. Moreover, full factorial and Taguchi methods are not appropriate for complex and nonlinear problems as higher-order empirical polynomial models

**Fig. 6.** (a) FDM tool path parameters, (b) build orientations, and (c) layer thickness.

cannot be developed using these design which is very important when the objective is optimization. Therefore, I-optimal design proposed in this study offer a good alternative approach, as it provides a better accuracy and precision with only 60 runs at 4–6 factor levels (irregular experimental matrix) including replications and extra unique model points to fit higher-order polynomials models. The precision and efficiency of an experimental design depends on the careful planning of the experimental procedures, as well as the accurate measurement of the responses. I-optimal design was performed in order to investigate the effects of the parameters involved on dimensional accuracy. I-optimal design suggested 38 runs for the six process parameters at different levels. Replications and extra unique model points were added in addition to the 38 runs to reduce the standard error, to test lack of fit, to improve the precision of developed models and to reduce the influence of design points (leverage) on the outcome of fitting regression. This provided an accurate estimate of the variation in the responses and provided the appropriate degrees of freedom required to develop adequate relationship between parameter and output responses. The final design matrix can be seen in **Table 3**.

3.2.3. Statistical modeling

The significance of factors and their interactions are evaluated with the ANOVA procedure using Fisher's *F*-test and *P*-value (probability value). The *F*-test value is determined by Eq. (2) [10]:

$$F = \frac{SS_R/k}{SS_E/(n - k - 1)} = \frac{MS_R}{MS_E} \quad (2)$$

where *F* represents *F*-test value; SS_E and SS_R represent a sum of squares due to the regression and a sum of squares due to the residual or error, respectively; MS_R denotes Mean Square Regression and MS_E denotes Mean Square Error (Residual); *k* denotes Degrees of Freedom for Regression and $n - k - 1$ denotes Total Degrees of Freedom for Error or Residual. If the *P*-value is smaller than 0.05, then the factor or interaction effect has a significant influence on the response and must be included in the predicted model.

There are five main criteria to check the adequacy of the regression model. The first criterion is R^2 , which measures how close the data are to the fitted line and it measures the amount of variability in the response *y* explained by variables *A, B, C...F*. The R^2 is determined by Eq. (3) [18]:

$$R^2 = 1 - \left[\frac{SS_{\text{residual}}}{(SS_{\text{residual}} + SS_{\text{model}})} \right]; \quad 0 \leq R^2 \leq 1 \quad (3)$$

where SS denotes sum of squares.

The second criterion is the adjusted R^2 . It measures the amount of variation around the mean explained by the model [18], which is defined in Eq. (4):

$$\text{Adj } R^2 = 1 - \left[\left(\frac{SS_{\text{residual}}}{df_{\text{residual}}} \right) / \left(\frac{SS_{\text{residual}} + SS_{\text{model}}}{df_{\text{residual}} + df_{\text{model}}} \right) \right]; \quad 0 \leq \text{Adj } R^2 \leq 1 \quad (4)$$

The third criterion is the predicted R^2 , which measures how well the model predicts a response value. Predicted R^2 is determined by Eq. (5) [15]:

$$\text{Pred } R^2 = 1 - \left[\frac{\text{PRESS}}{(SS_{\text{residual}} + SS_{\text{model}})} \right]; \quad 0 \leq \text{Pred } R^2 \leq 1 \quad (5)$$

where PRESS is the predicted residual error sum of squares, and it measures how the regression model fits each design point. The smaller the PRESS statistic, the better the model fits the data points. The difference between Predicted R^2 and Adj R^2 must be less than 0.2. If the difference is more than 0.2, this means that there is a problem either in the data or in the model selected.

The fourth criterion is the lack-of-fit test, which compares the residual error to the pure error from the replicated design points in order to evaluate whether the model adequately fits the response data [19]. The lack-of-fit value is tested against the pure error, which is expected to be not significant for a good fit. Lack-of-fit could be considered as insignificant if *P*-value is larger than 0.05 (Probability > 0.05). If the *P*-value is smaller than the level of significance (0.05), then the lack-of-fit will be considered as significant and hence the model will not qualify to fit the data appropriately.

The final criterion is adequacy precision. Adequacy precision measures the signal-to-noise ratio of the experimental data. It compares the predicted values, \hat{Y} and the average prediction error, \bar{V} at the design points. A ratio greater than 4 is desirable. The adequacy precision is determined by Eq. (6) [20]:

$$\begin{aligned} \text{Adeq Precision} &= \left[\frac{\max(\hat{Y}) - \min(\hat{Y})}{\sqrt{\bar{V}(\hat{Y})}} \right] > 4\bar{V}(\hat{Y}) \\ &= \frac{1}{n} \sum_{i=1}^n \bar{V}(\hat{Y}) = \frac{p\sigma^2}{n} \end{aligned} \quad (6)$$

where *p* is number of model parameters, σ^2 is residual mean square, and *n* is number of experiments.

4. Analysis

According to the I-optimal design matrix, percentage dimensional changes in terms of length, width and thickness analyses were performed to obtain the values of the different response variables and to investigate the effects of the parameters involved. **Table 3** presents the experimental results for percentage changes in length (ΔL), width (ΔW) and thickness (ΔT) under each set of operating conditions based on I-optimal design. The responses obtained from the experiments were then analyzed to develop the mathematical models with best fits. JMP and Design Expert software's were used for regression and graphical analysis of the data collected from experimentation. In this study, linear, two-factor interaction (2FI), quadratic and cubic models were analyzed. In order to determine the best model in terms of its ability to fit the experimental data, three different tests – the sequential model sum of squares, lack-of-fit, and the model adequacy – were conducted. The statistical summary of the models is

Table 3

I-optimal design matrix and collected data.

Run	Factors						Responses			Desirability index
	A	B	C	D	E	F	ΔL	ΔW	ΔT	
1	0.2540	0.5	90	90	0.4572	1	0.1714	0.5280	2.1905	0.945
2	0.2540	0.3	45	45	0.5298	5	0.1886	0.7520	4.3429	0.975
3	0.2540	0.3	45	45	0.5298	5	0.2000	0.7200	4.3686	0.959
4	0.3302	0.4	90	30	0.4814	1	0.1343	0.6400	6.0000	0.951
5	0.1270	0.2	45	90	0.4572	1	0.0714	-0.1200	2.5714	0.949
6	0.2540	0.2	45	90	0.4572	5	0.1571	0.5200	5.0286	0.938
7	0.1270	0	0	45	0.4572	5	0.0786	0.1064	4.2857	0.949
8	0.3302	0.5	0	90	0.4814	1	0.0571	0.6200	8.2857	0.946
9	0.3302	0	90	90	0.4572	8	-0.0571	0.3040	12.3800	0.000
10	0.1270	0	45	0	0.5056	7	-0.1200	0.3400	4.8571	0.853
11	0.3302	0.5	90	0	0.5782	1	0.1800	0.6600	6.0571	0.966
12	0.3302	0.2	0	90	0.4572	10	0.1029	0.5400	10.1143	0.866
13	0.3302	0.3	90	0	0.4572	7	0.1000	0.6880	7.2857	0.944
14	0.1778	0.5	0	0	0.4572	1	-0.0571	0.4000	3.8286	0.950
15	0.1270	0	90	45	0.4572	10	-0.0143	0.1400	4.6857	0.957
16	0.1270	0.5	90	75	0.5056	5	0.1000	0.1600	2.5714	0.991
17	0.1270	0.5	90	0	0.5782	10	-0.0794	0.3400	2.6286	0.113
18	0.3302	0	90	60	0.4814	1	-0.0857	0.4800	11.1800	0.958
19	0.1270	0.2	45	45	0.5782	10	0.1071	0.3000	2.3429	0.933
20	0.1270	0.5	30	75	0.5540	8	0.0571	0.1200	3.9143	0.854
21	0.3302	0	30	0	0.4572	1	-0.1357	0.2800	7.7143	0.921
22	0.2540	0.5	90	90	0.4572	10	0.1429	0.5760	3.2886	0.727
23	0.1270	0	90	90	0.5782	3	0.0943	0.2400	3.4286	0.943
24	0.3302	0	30	45	0.5298	10	0.0657	0.6000	12.2857	0.000
25	0.1778	0	90	0	0.5298	1	-0.1714	0.3000	4.0000	0.950
26	0.2540	0.5	90	75	0.5540	1	0.2071	0.6600	2.9714	0.000
27	0.1778	0.5	60	0	0.4572	10	0.0571	0.5600	3.2571	0.881
28	0.1778	0	0	90	0.5056	1	0.1514	0.2200	5.2571	0.935
29	0.2540	0.3	45	45	0.5298	5	0.1714	0.7200	4.8571	0.797
30	0.1270	0.3	0	0	0.5298	7	-0.0857	0.2400	3.4286	0.942
31	0.3302	0.5	45	45	0.4572	10	0.1429	0.8000	8.9714	0.911
32	0.3302	0.5	90	90	0.5782	10	0.0286	0.6000	8.6286	0.970
33	0.3302	0.5	0	0	0.5782	10	-0.0571	0.7680	9.7143	0.963
34	0.3302	0.2	60	90	0.5782	1	0.1314	0.6640	8.5143	0.957
35	0.2540	0.5	0	90	0.5782	7	0.0571	0.6080	4.5714	0.948
36	0.3302	0.2	0	0	0.5782	1	0.0571	0.5200	7.0286	0.895
37	0.3302	0	0	60	0.5782	5	0.1071	0.7120	11.4286	0.904
38	0.2540	0.3	45	45	0.5298	5	0.1857	0.7360	4.8000	0.966
39	0.1270	0.5	0	90	0.5782	1	0.0929	0.1600	3.4857	0.849
40	0.2540	0.3	45	45	0.5298	5	0.1857	0.7520	4.3429	0.965
41	0.2540	0	45	90	0.5056	7	0.1143	0.4800	8.5000	0.947
42	0.1270	0	45	0	0.5056	7	-0.0857	0.1800	4.1143	0.899
43	0.1778	0.5	45	30	0.5782	1	0.0929	0.4800	2.9143	0.853
44	0.1270	0.2	45	45	0.5782	10	0.0857	0.1600	3.4057	0.644
45	0.1270	0	0	0	0.5782	1	-0.0571	0.2400	2.7143	0.945
46	0.2540	0	0	0	0.4572	10	0.0657	0.6720	5.2571	0.963
47	0.1270	0.3	90	0	0.4572	1	-0.2286	0.0800	3.1429	0.815
48	0.2540	0.3	90	30	0.5056	10	0.1643	0.7200	4.8571	0.891
49	0.1778	0	0	90	0.5782	10	0.1143	0.3200	4.6571	0.878
50	0.1778	0.3	90	90	0.5298	10	0.0857	0.2664	2.5714	0.778
51	0.2540	0.1	90	30	0.5782	5	0.1857	0.7840	4.8000	0.831
52	0.2540	0.3	45	45	0.5298	5	0.1786	0.7040	4.4571	0.829
53	0.3302	0.2	60	90	0.5782	1	0.0720	0.6160	8.8571	0.843
54	0.3302	0	90	0	0.5782	10	0.0857	0.8160	11.6000	0.966
55	0.2540	0.3	0	45	0.4572	5	0.1914	0.7200	4.5714	0.772
56	0.1270	0.3	0	45	0.5056	10	0.0714	0.2800	3.6514	0.959
57	0.3302	0.5	45	0	0.5056	5	0.0857	0.7600	7.1429	0.958
58	0.1270	0.4	15	60	0.5056	3	0.0762	0.1600	4.1143	0.894
59	0.1270	0.5	15	90	0.4572	10	0.0571	0.0960	3.1057	0.929
60	0.2540	0.3	45	45	0.5298	5	0.2000	0.7200	4.8571	0.946

shown in Table 4. From this table, it is clear that the quadratic model has the highest R^2 , adjusted R^2 and predicted R^2 . In addition, adjusted R^2 and predicted R^2 are in very good agreement with each other. Moreover, the quadratic

model has smaller p -values (significance) and PRESS with insignificant lack-of-fit in comparison with the other models. Therefore, the quadratic model provides an excellent explanation for the relationship between FDM parameters

Table 4

The statistical summary of the models.

Response	Model	Sequential P-value	Lack of fit P-value	R^2	R_{Adj}^2	R_{Pred}^2	PRESS	Precision	Remarks
(ΔL)	Linear	0.0029	<0.0001	0.3038	0.2250	0.0906	0.56	Inadequate	
	2FI	0.0026	<0.0001	0.6856	0.5119	-0.0503	0.65	Inadequate	
	Quadratic	<0.0001	0.5495	0.9816	0.9661	0.9070	0.057	Adequate	Selected
	Cubic	0.5495	N/A	0.9655	0.9655	**	**	Inadequate	Aliased
(ΔW)	Linear	<0.0001	0.0013	0.7125	0.6800	0.6370	1.26	Inadequate	
	2FI	0.2859	0.0015	0.8070	0.7004	0.4862	1.78	Inadequate	
	Quadratic	<0.0001	0.7862	0.9798	0.9627	0.9127	0.30	Adequate	Selected
	Cubic	0.7862	N/A	0.9926	0.9513	**	**	Inadequate	Aliased
(ΔT)	Linear	<0.0001	<0.0001	0.7558	0.7282	0.6814	143.70	Inadequate	
	2FI	0.1127	<0.0001	0.8512	0.7690	0.5860	186.75	Inadequate	
	Quadratic	<0.0001	0.4756	0.9893	0.9804	0.9550	20.29	Adequate	Selected
	Cubic	0.4756	N/A	0.9972	0.9815	**	**	Inadequate	Aliased

N/A: not applicable.

** Case(s) with leverage of 1.0000: predicted R^2 and PRESS statistic not defined.

and dimensional accuracy and it was therefore used in this study. Although the cubic model contains linear, two-factor terms and three-factor terms (highest polynomial model), it was not selected because it is aliased.

4.1. Development of mathematical models

To develop the mathematical models, a quadratic regression model was used in this study to establish a relationship between the independent variables (X_i) and the output responses (Y). The quadratic regression model used in this study can be expressed as in Eq. (7).

$$Y = \beta_0 + \sum_{i=1}^k \beta_i X_i + \sum_{i=1}^k \beta_{ii} X_i^2 + \sum_{i < j} \beta_{ij} X_i X_j + \varepsilon \quad (7)$$

where Y denotes the predicted response, X_i and X_j are the coded variables, k is total number of variables, β_0 is the constant term of the regression equation, β_i is the linear coefficient, β_{ii} is the squared term of each variable, β_{ij} is the interactive coefficient, and ε is the random error, which contains measurement error and other variability.

And for six parameters, the quadratic model could be expressed in Eq. (8).

$$\begin{aligned} Y = & \beta_0 + \beta_1 A + \beta_2 B + \beta_3 C + \beta_4 D + \beta_5 E + \beta_6 F + \beta_{12} AB \\ & + \beta_{13} AC + \beta_{14} AD + \beta_{15} AE + \beta_{16} AF + \beta_{23} BC \\ & + \beta_{24} BD + \beta_{25} BE + \beta_{26} BF + \beta_{34} CD + \beta_{35} CE \\ & + \beta_{36} CF + \beta_{45} DE + \beta_{46} DF + \beta_{56} EF + \beta_{11} A^2 + \beta_{22} B^2 \\ & + \beta_{33} C^2 + \beta_{44} D^2 + \beta_{55} E^2 + \beta_{66} F^2 \end{aligned} \quad (8)$$

After determining the coefficients, the mathematical models were developed. These models can be used for studying and evaluation the relationship between input parameters and the required dimensional accuracy as a percentage change in length, width, and thickness by giving levels of each factor, where the levels of the factors should be specified in the original units. The final developed models, in terms of actual values for percentage change in length (ΔL), width (ΔW), and thickness (ΔT), are given by Eqs. (9)–(11), respectively.

$$\begin{aligned} \Delta L(\%) = & 0.080214 + 3.34289A + 1.13258B \\ & - 6.07680 \times 10^{-3}C + 9.73988 \times 10^{-3}D \\ & - 3.39576E + 0.084496F + 0.75602AB \\ & + 3.62491 \times 10^{-3}AC - 0.010804AD \\ & + 3.50045 \times 10^{-3}BC - 5.81221 \times 10^{-4}BD \\ & - 1.82709 * BE - 0.021960BF - 5.00277 \\ & \times 10^{-6}CD + 8.21725 \times 10^{-3}CE + 5.27659 \\ & \times 10^{-5}CF - 4.60899 \times 10^{-3}DE - 1.30511 \\ & \times 10^{-4}DF - 0.11027EF - 6.44425A^2 \\ & - 0.57895B^2 - 3.05067 \times 10^{-5}D^2 \\ & + 4.41203E^2 - 1.50096 \times 10^{-3}F^2 \end{aligned} \quad (9)$$

$$\begin{aligned} \Delta W(\%) = & -2.03901 + 9.89835A + 1.85945B \\ & - 4.52642 \times 10^{-3}C + 2.21223E \times 10^{-3}D \\ & + 2.13752E + 0.11488F + 1.17147AB \\ & + 4.90693 \times 10^{-3}AD - 3.70552BE \\ & + 8.69044 \times 10^{-3}CE - 2.98283 \times 10^{-4}DF \\ & - 0.12238EF - 17.75156A^2 - 3.57785 \\ & \times 10^{-5}D^2 - 2.59847 \times 10^{-3}F^2 \end{aligned} \quad (10)$$

$$\begin{aligned} \Delta T(\%) = & -29.05106 - 103.61701A - 2.43897B \\ & + 9.46291 \times 10^{-3}C + 8.92274 \times 10^{-3}D \\ & + 163.10189E - 0.15845F - 24.21662AB \\ & + 0.11539AD + 54.47932AE + 1.18620AF \\ & - 0.048185BC - 0.045592BD - 8.57306 \\ & \times 10^{-5}CD + 213.22914A^2 + 16.72849B^2 \\ & - 1.42849 \times 10^{-4}D^2 - 169.33223E^2 \end{aligned} \quad (11)$$

All developed mathematical models are subject to constraints:

$$\begin{aligned} 0.1270 \text{ mm} & \leq A \leq 0.3302 \text{ mm} \\ 0 & \leq B \leq 0.5 \text{ mm} \end{aligned}$$

$$\begin{aligned}0^\circ \leq C \leq 90^\circ \\ 0^\circ \leq D \leq 90^\circ \\ 0.4572 \text{ mm} \leq E \leq 0.5782 \text{ mm} \\ 1 \leq F \leq 10.\end{aligned}$$

4.2. Checking of data and adequacy of developed models

The adequacy of the developed models was tested at 95% confidence interval by employing the ANOVA technique, which is used to test the significance of the developed models. In order to develop realistic models, insignificant terms with the highest partial probability values were eliminated from the models using the backward elimination method, as it fits the data appropriately. The ANOVA results for the reduced quadratic models for percentage changes in length, width, and thickness are shown in Tables 5–7, respectively, where it can be seen that the probability value (*P*-value) for all models is smaller than 0.05, indicating that the terms in the model have significant effect on the output responses. It confirms that the developed models have 95% confidence level. Meanwhile, the lack-of-fit for all models is statistically not significant relative to pure error, as the *P*-values of 0.4890, 0.8478, and 0.5934 for all models are more than 0.05 (Probability > 0.05). Tables 5–7 also show the other adequacy measures – R^2 , adjusted R^2 , and predicted R^2 . For all the

developed models, the values of the coefficient of determination, that is, R^2 , adjusted R^2 , and predicted R^2 , was found to be very close to 1, indicating a high precision, good fit, and perfect correlation between the predicted and the experimental values. The adequate precision ratios for all models are considerably greater than 4 (Adequate Precision > 4), which indicates an adequate signal for the developed models discrimination. Furthermore, Tables 5–7 show prediction error sum of squares (PRESS). In all cases, these values of PRESS are substantially smaller, which implies high precision and reliability of the developed models.

The validity of the developed regression models was also checked through normal probability plots. The normal probability plots of residuals for percentage change in length, width, and thickness are shown in Fig. 7(a–c), respectively. These figures indicate that the residuals follow a normal distribution and lie on a straight line, which indicates that the errors are normally distributed and the developed models are well fitted with the experimental values. The predicted values of percentage change in length, width, and thickness using developed models, given in Eqs. (9)–(11), were compared with the experimental values. The experimental values were plotted together with the predicted values for three responses, respectively, presented in Fig. 8(a–c). It can be seen that there is high degree of correlation between the experimental values

Table 5
ANOVA test results for percentage change in length.

Source	Sum of squares	DOF	Mean square	F-value	P-value	Remarks At 95% CI
Model	0.60	24	0.025	66.35	<0.0001	Significant
<i>A</i> – Layer thickness	0.026	1	0.026	68.73	<0.0001	Significant
<i>B</i> – Air gap	0.014	1	0.014	37.69	<0.0001	Significant
<i>C</i> – Raster angle	2.062×10^{-4}	1	2.062×10^{-4}	0.55	0.4652	Not Significant
<i>D</i> – Build orientation	0.078	1	0.078	207.27	<0.0001	Significant
<i>E</i> – Road width	9.822×10^{-3}	1	9.822×10^{-3}	25.98	<0.0001	Significant
<i>F</i> – Number of contours	2.643×10^{-3}	1	2.643×10^{-3}	6.99	0.0122	Significant
<i>AB</i>	9.153×10^{-3}	1	9.153×10^{-3}	24.21	<0.0001	Significant
<i>AC</i>	6.614×10^{-3}	1	6.614×10^{-3}	17.49	0.0002	Significant
<i>AD</i>	0.061	1	0.061	160.59	<0.0001	Significant
<i>BC</i>	0.038	1	0.038	99.87	<0.0001	Significant
<i>BE</i>	0.019	1	0.019	49.96	<0.0001	Significant
<i>BF</i>	0.015	1	0.015	39.34	<0.0001	Significant
<i>CD</i>	2.571×10^{-3}	1	2.571×10^{-3}	6.80	0.0133	Significant
<i>CE</i>	0.013	1	0.013	34.47	<0.0001	Significant
<i>CF</i>	2.926×10^{-3}	1	2.926×10^{-3}	7.74	0.0086	Significant
<i>DE</i>	4.159×10^{-3}	1	4.159×10^{-3}	11.00	0.0021	Significant
<i>DF</i>	0.018	1	0.018	47.94	<0.0001	Significant
<i>EF</i>	0.025	1	0.025	66.15	<0.0001	Significant
<i>A</i> ²	0.041	1	0.041	107.73	<0.0001	Significant
<i>B</i> ²	0.014	1	0.014	35.92	<0.0001	Significant
<i>D</i> ²	0.036	1	0.036	96.16	<0.0001	Significant
<i>E</i> ²	2.332×10^{-3}	1	2.332×10^{-3}	6.17	0.0180	Significant
<i>F</i> ²	8.392×10^{-3}	1	8.392×10^{-3}	22.19	<0.0001	Significant
Residual	0.013	35	3.781×10^{-4}	–	–	–
Lack of Fit	9.994×10^{-3}	26	3.844×10^{-4}	1.07	0.4890	Not significant
Pure error	3.240×10^{-3}	9	3.600×10^{-4}	–	–	–
Cor. total	0.62	59	–	–	–	–
Std. dev = 0.019				$R^2 = 0.9785$		
Mean = 0.071				Adjusted $R^2 = 0.9637$		
CV (%) = 27.29				Predicted $R^2 = 0.9255$		
PRESS = 0.046				Adequacy precision = 33.355		

Table 6

ANOVA test results for percentage change in width.

Source	Sum of squares	DOF	Mean square	F-value	P-value	Remarks At 95% CI
Model	3.38	15	0.23	112.50	<0.0001	Significant
A – Layer thickness	2.05	1	2.05	1023.82	<0.0001	Significant
B – Air gap	0.096	1	0.096	48.13	<0.0001	Significant
C – Raster angle	5.372×10^{-5}	1	5.372×10^{-5}	0.027	0.8706	Not significant
D – Build orientation	0.17	1	0.17	83.67	<0.0001	Significant
E – Road width	0.12	1	0.12	58.01	<0.0001	Significant
F – Number of contours	0.068	1	0.068	34.08	<0.0001	Significant
AB	0.023	1	0.023	11.24	0.0017	Significant
AD	0.013	1	0.013	6.41	0.0150	Significant
BE	0.079	1	0.079	39.47	<0.0001	Significant
CE	0.015	1	0.015	7.33	0.0096	Significant
DF	0.098	1	0.098	48.72	<0.0001	Significant
EF	0.031	1	0.031	15.64	0.0003	Significant
A ²	0.33	1	0.33	164.80	<0.0001	Significant
D ²	0.058	1	0.058	29.12	<0.0001	Significant
F ²	0.028	1	0.028	14.17	0.0005	Significant
Residual	0.088	44	2.002×10^{-3}	–	–	–
Lack of Fit	0.062	35	1.781×10^{-3}	0.62	0.8478	Not significant
Pure Error	0.026	9	2.859×10^{-3}	–	–	–
Cor. total	3.47	59	–	–	–	–
Std. dev = 0.045				$R^2 = 0.9746$		
Mean = 0.47				Adjusted $R^2 = 0.9659$		
CV (%) = 9.52				Predicted $R^2 = 0.9493$		
PRESS = 0.18				Adequacy precision = 37.905		

Table 7

ANOVA test results for percentage change in thickness.

Source	Sum of squares	DOF	Mean square	F-value	P-value	Remarks at 95% CI
Model	445.45	17	26.20	195.83	<0.0001	Significant
A – Layer thickness	293.25	1	293.25	2191.61	<0.0001	Significant
B – Air gap	32.59	1	32.59	243.52	<0.0001	Significant
C – Raster angle	2.97	1	2.97	22.22	<0.0001	Significant
D – Build orientation	3.70	1	3.70	27.68	<0.0001	Significant
E – Road width	7.060×10^{-3}	1	7.060×10^{-3}	0.053	0.8194	Not significant
F – Number of contours	9.48	1	9.48	70.88	<0.0001	Significant
AB	9.44	1	9.44	70.54	<0.0001	Significant
AD	6.95	1	6.95	51.97	<0.0001	Significant
AE	2.98	1	2.98	22.24	<0.0001	Significant
AF	7.63	1	7.63	57.04	<0.0001	Significant
BC	7.27	1	7.27	54.30	<0.0001	Significant
BD	6.83	1	6.83	51.02	<0.0001	Significant
CD	0.77	1	0.77	5.76	0.0209	Significant
A ²	46.69	1	46.69	348.97	<0.0001	Significant
B ²	11.44	1	11.44	85.48	<0.0001	Significant
D ²	0.82	1	0.82	6.16	0.0171	Significant
F ²	3.80	1	3.80	28.40	<0.0001	Significant
Residual	5.62	42	0.13	–	–	–
Lack of Fit	4.35	33	0.13	0.93	0.5934	Not significant
Pure error	1.27	9	0.14	–	–	–
Cor total	451.07	59	–	–	–	–
Std. dev = 0.37				$R^2 = 0.9875$		
Mean = 5.50				Adjusted $R^2 = 0.9825$		
CV (%) = 6.65				Predicted $R^2 = 0.9727$		
PRESS = 12.34				Adequacy precision = 52.828		

and predicted values, which indicates that the developed models are able to accurately describe the relationship between parameters and dimensional accuracy and can produce accurate results.

5. Results and discussion

In order to understand the effect of the process parameters on the output responses, the 3-D response surface

plots can be used graphically to study the interactions between the factors and their main effects on the responses, while the other variables are held constant at their center level. In addition, 3-D response surface plots can be used to find the optimum response of percentage change in length, width, and thickness. The 3-D surface graphs were plotted by applying the developed models in order to understand the behavior of the output responses, which are affected by different levels of process parame-

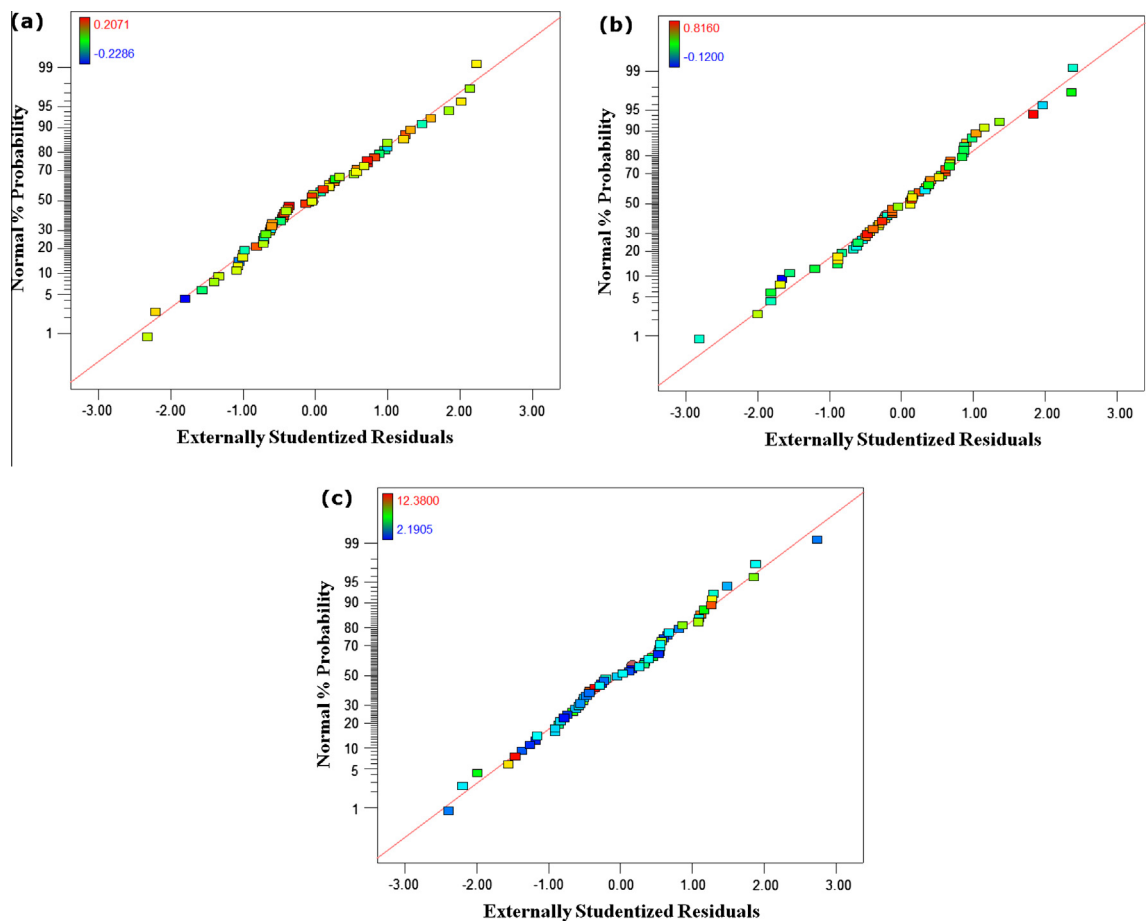


Fig. 7. Normal probability plot of residuals for percentage change in: (a) length, (b) width, and (c) thickness.

ters. Figs. 9–11 show the corresponding 3-D response surface plots representing various interactive effects of parameters for the three required output responses comprising percentage changes in length, width, and thickness respectively. In Figs. 9–11, the colored bars indicate the various effects of process variables on the required response. From these figures, it can be seen that the layer thickness was the most critical factor affecting all responses. Therefore, the relationship between layer thickness and other parameters are studied further in all 3-D surface plots.

5.1. Influence of process parameter on percentage change in length

A high interaction between various process parameters for percentage change in length was observed. The 3D surface plots between the most significant process parameter interactions for percentage change in length is shown in Fig. 9(a–e). It can be observed from Fig. 9(a) that percentage change in length between the fabricated part and the designed dimension can be reduced by decreasing the layer thickness and increasing the air gap between rasters. The percentage change in length is found to be less

(0.0498%) for minimum layer thickness of 0.127 mm with zero air gap between rasters. The effect of layer thickness and build orientation on percentage change in length is shown in Fig. 9(b) with air gap, raster angle, road width, and number of contours held constant at their midpoint. Dimensional inaccuracy can happen as a result of the shrinkage of extruded material when it cools down from a semi-molten state to the solid state. It can be noted in Fig. 9(b) that percentage change became a negative value. A negative value of percentage change means there is shrinkage in the part, meaning that the experimental value is less than the designed value. Conversely, a positive value of percentage change means there is expansion in the part's dimensions, which means the value of response is greater than the designed value. From this figure, it is clear that there is shrinkage (-0.0759%) along the length when the level of layer thickness and build orientation decreases from a high to a low level. The optimum value of percentage change in length (0.0008%) for this interaction can be obtained with a layer thickness of 0.127 mm and build orientation around 17° .

Fig. 7(c) shows the response surface plot of the effect of layer thickness and number of contours on percentage change in length when other parameters remain constant

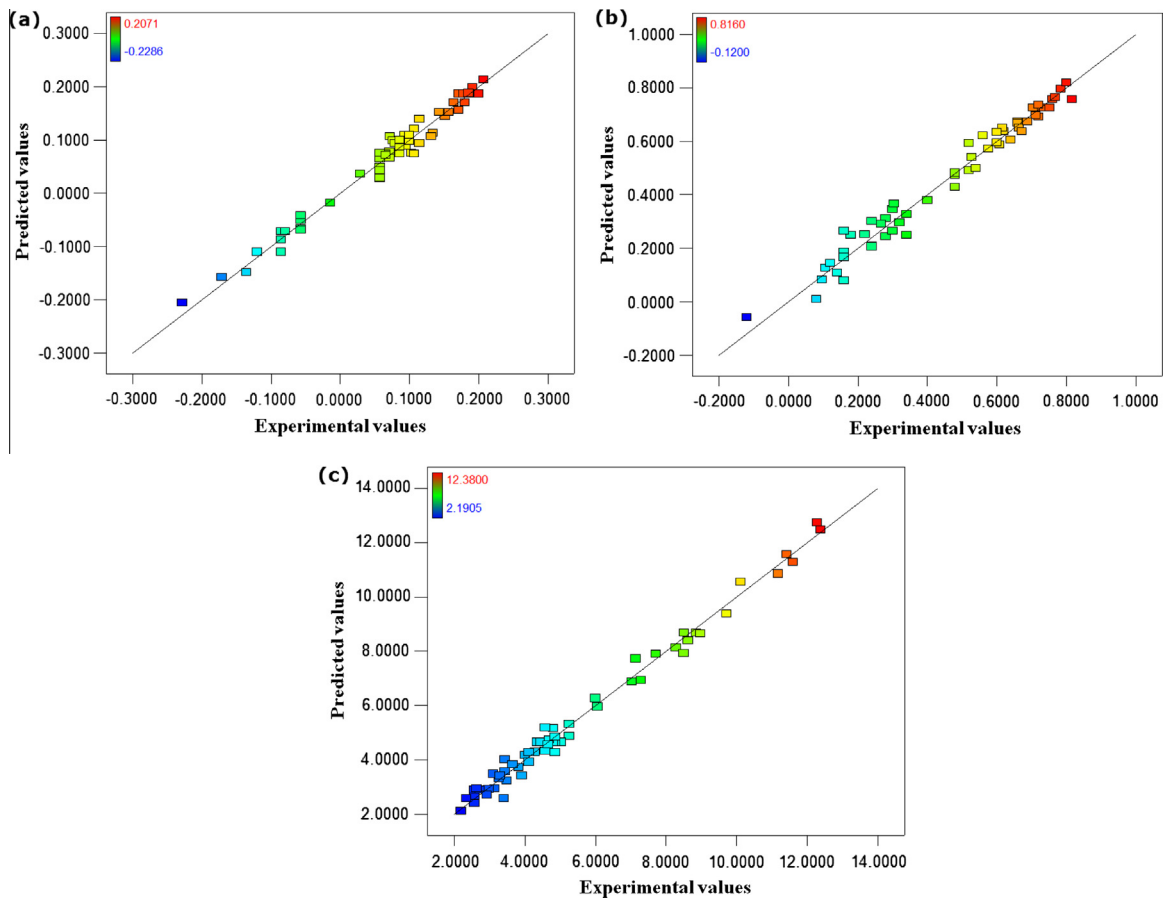


Fig. 8. Comparisons of predicted and experimental values for percentage change in: (a) length, (b) width, and (c) thickness.

at their midpoint. As it seen from this figure, percentage change in length tends to increase steadily with an increase in layer thickness and slightly by increase in number of contours. From this surface plot, it can be noticed that the optimum value of percentage change in length (0.0459%) for this interaction can be achieved by decreasing the layer thickness from 0.3302 to 0.127 mm and the number of contours from 10 to 1. This is because the lower values of number of contours can reduce the deformation by reducing thermal stress accumulation. Fig. 9(d) shows the effect of raster angle and layer thickness on percentage change in length. It was observed that the percentage change decreased as the raster angle increased to its highest level (90°) and decreased as the layer thickness decreased to its lowest level (0.127 mm). The percentage change in length was found to be the least (0.0631%) for the minimum layer thickness (0.127 mm) and maximum value of raster angle (90°). It is well known that the highest value of raster angle is preferable. This is due to the latter resulting in shorter rasters, smaller curves, and smaller sharp angles, thereby reducing the non-uniform temperature gradients and thermal stresses.

Road width has a marginal effect on percentage change in length, as shown in Fig. 9(e), but layer thickness has a significant effect on this response. The result indicates that percentage change in length for this interaction effect can

be improved by using the minimum value of both road width and layer thickness. This is so because the use of the highest value of road width along with the highest value of layer thickness can result in inner stresses. The inner stresses are a result of the cooling phase during the change from the glass transition temperature to the chamber temperature [21]. This inner stress is the main cause of distortion and deformation in the outside edges of the part, which affect part accuracy. The optimum value (0.0799%) of percentage change in length for this interaction effect can be obtained with layer thickness of 0.127 mm and road width of 0.4572 mm.

5.2. Influence of process parameter on percentage change in width

Fig. 10(a-e) shows the response surface plots of the effect of the most significant interactive terms on percentage change in width. It can be observed from Fig. 10(a) that percentage change in width decreased significantly with decrease in layer thickness, but it reduced only slightly with decrease in air gap between adjacent rasters. The minimum percentage change in width (0.2246%) occurs for this interaction at the lower value of layer thickness and air gap. The effect of layer thickness and build orientation on percentage change in width is shown Fig. 10(b). As

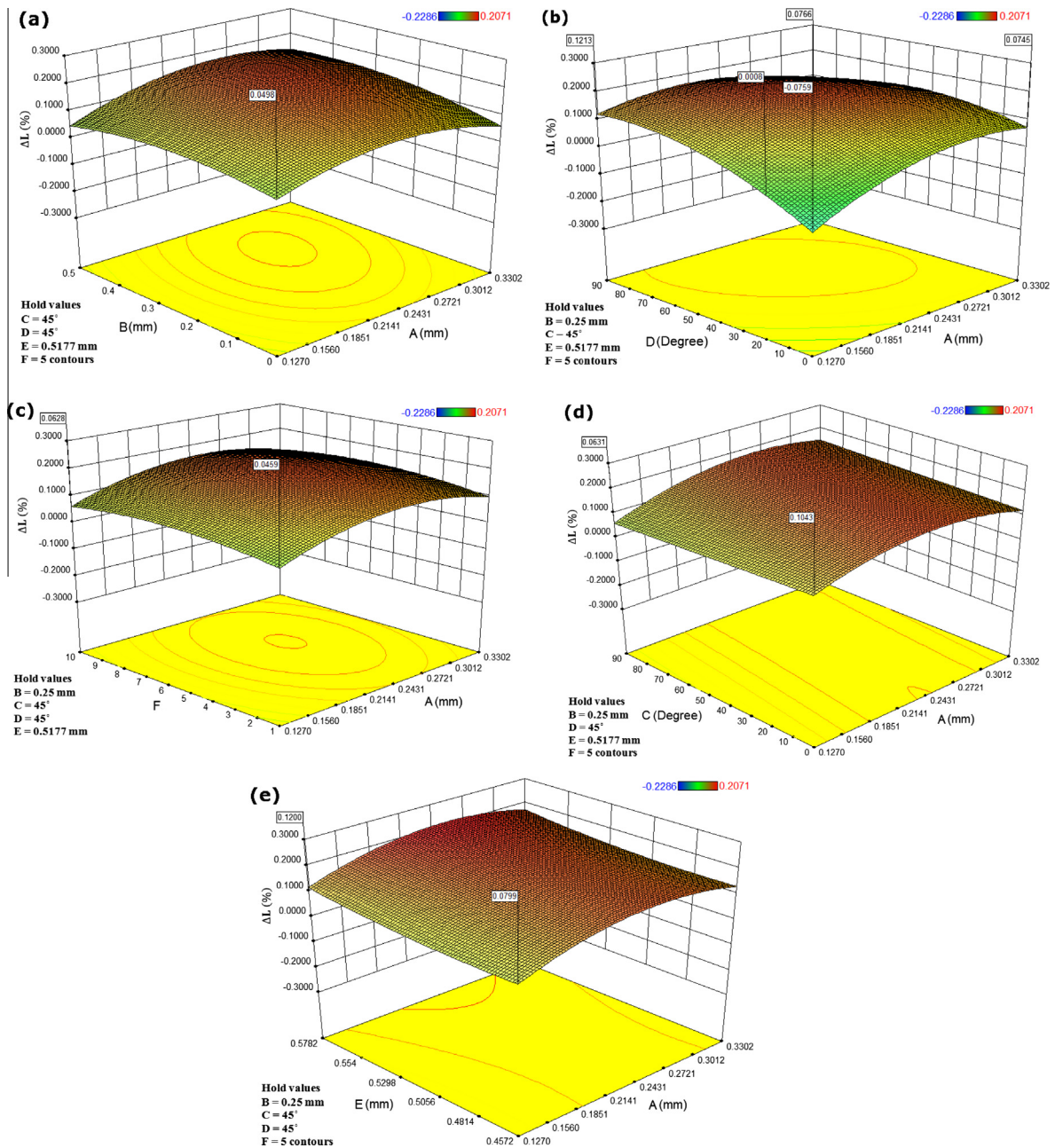


Fig. 9. 3D response surface plots representing various interactive effects of parameters on percentage change in length.

seen from this figure, percentage change in width decreases linearly with increase in build orientation and decrease in layer thickness. It exhibited a decrease to the minimum value (0.085%) for the minimum layer thickness of 0.127 mm and the highest value of build orientation (90°). Fig. 10(c) shows the influence of layer thickness and number of contours on percentage change in width. This figure indicates that the value of percentage change in width increases much as the layer thickness increases and very slightly as the number of contours increases. The surface plot shows that percentage change in width can be reduced from 0.7033% to 0.1523% by

decreasing layer thickness from 0.3302 mm to 0.127 mm and number of contours from 10 to 1. Response surface graphs for both layer thickness versus raster angle and layer thickness versus road width are presented in Fig. 10 (d and e). It can be noticed that percentage change in width decreases at the higher values of raster angle (see Fig. 10 (d)) and at the lower values of road width (see Fig. 10(e)) as layer thickness decreases from 0.3302 to 0.127 mm. It is also observed from Fig. 10(d) that the minimum percentage change in width (0.2433%) occurs at the highest raster angle and minimum layer thickness. Similarly, minimum percentage change in width (0.1809%) for interaction effect

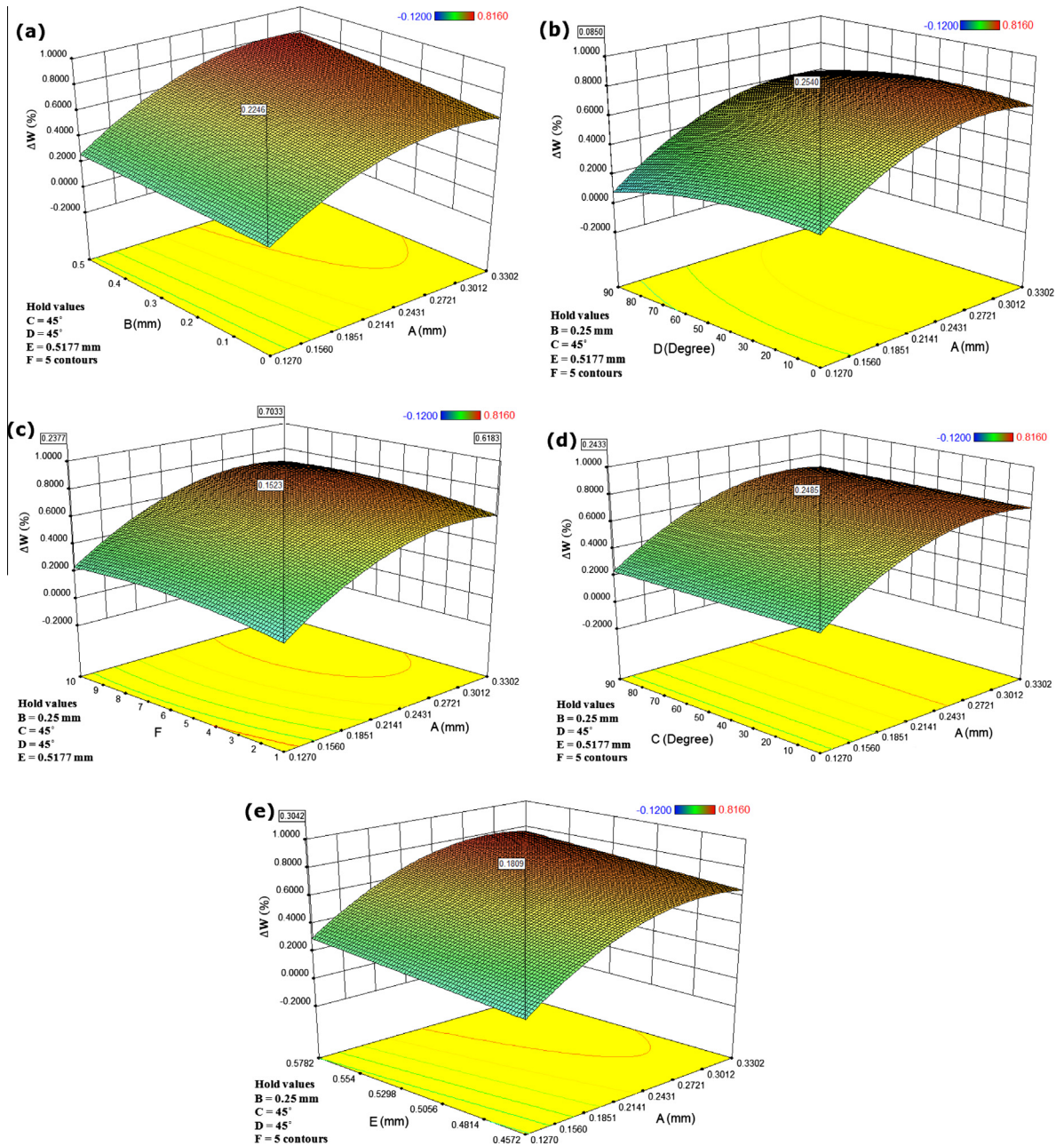


Fig. 10. 3D response surface plots representing various interactive effects of parameters on percentage change in width.

between layer thickness and road width can be obtained at the minimum value of road width and layer thickness, as shown in Fig. 10(e). This may be due to the residual stress concentration increasing with the increase in road width and layer thickness.

5.3. Influence of process parameter on percentage change in thickness

Fig. 11(a) shows the 3D response surface graph between layer thickness and air gap for percentage change in thickness. From this figure, it can be observed that percentage

change in thickness of the part decreases linearly in relation to decrease in layer thickness and increase in air gap. This is so because a high value of air gap helps to prevent the formation of the part between rasters, and thus reduces the percentage change in thickness of the manufactured part. The optimal value of percentage change in thickness (3.0735%) for this interaction occurs at layer thickness 0.1788 mm and air gap 0.3 mm. It is observed experimentally that thick layers with zero air gap can degrade the part's surface, causing deformation and overfill between rasters, and hence increasing the dimensional deviations between the experimental value and designed

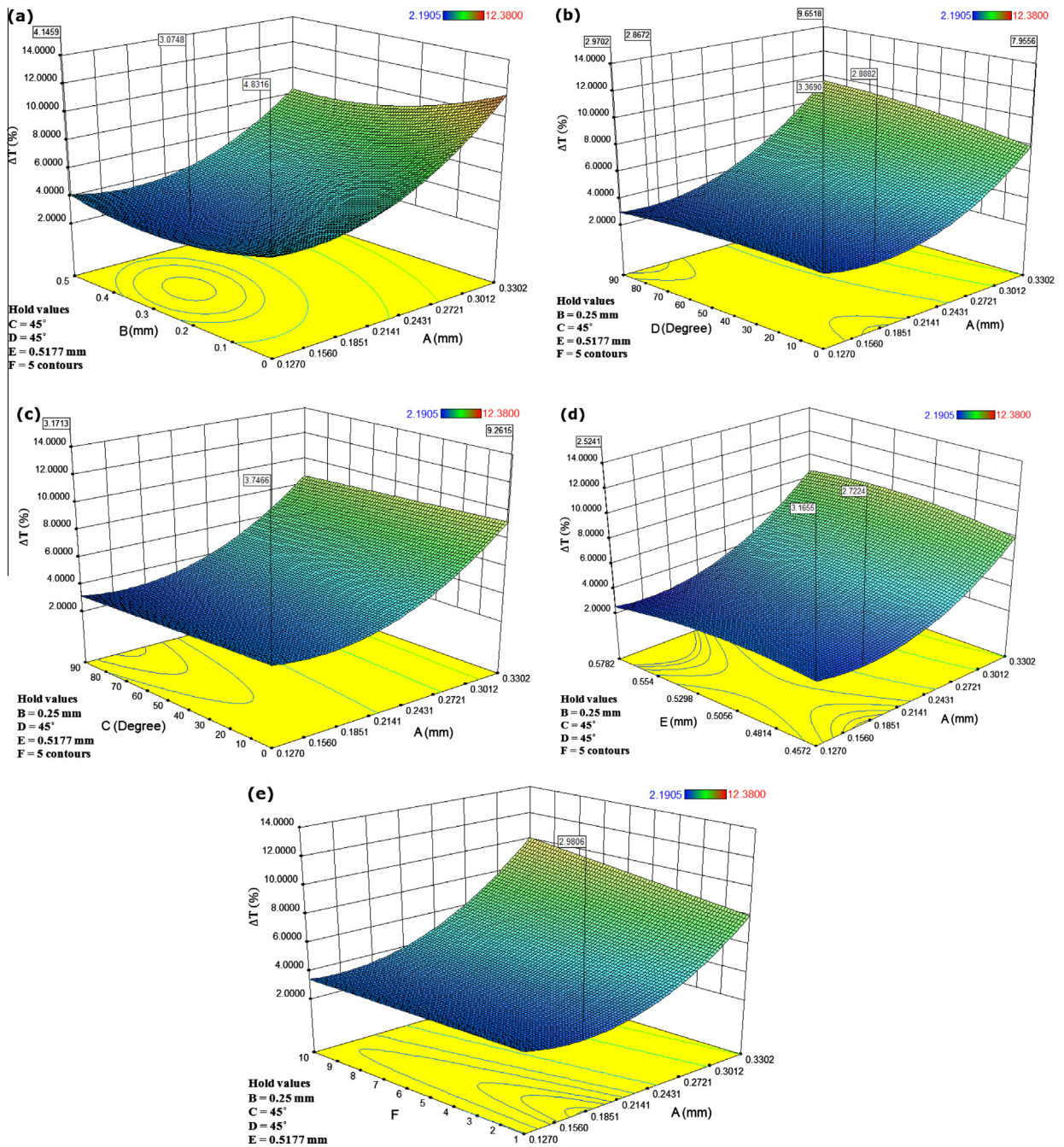


Fig. 11. 3D response surface plots representing various interactive effects of parameters on percentage change in thickness.

value. Unlike the length and width, where shrinkage and expansion occurred in some fabricated parts, the thickness of all fabricated parts was more than the designed value (thickness > 3.5 mm), which seems to be more vulnerable to dimensional errors due to height error along Z direction and variable changes. For example, in this study, all parts need to be manufactured with height (H) of 3.5 mm and some of these parts need to be manufactured with slicing thickness (T) of 0.127 mm, so the number of layers (n)

required to build this part is 27.56 layers. However, if the part needs to be fabricated with the same height, but with a higher value of slice thickness, such as 0.3302 mm, then the number of layers (n) required is 10.60 layers. Thus, 27 and 10 layers, in the case of using slicing thickness 0.127 mm and 0.3302 mm, respectively, will be deposited normally because of the constant extruded filament flow rate. However, 0.56 and 0.60 are the number of layers remaining to be fabricated or deposited and, in this case,

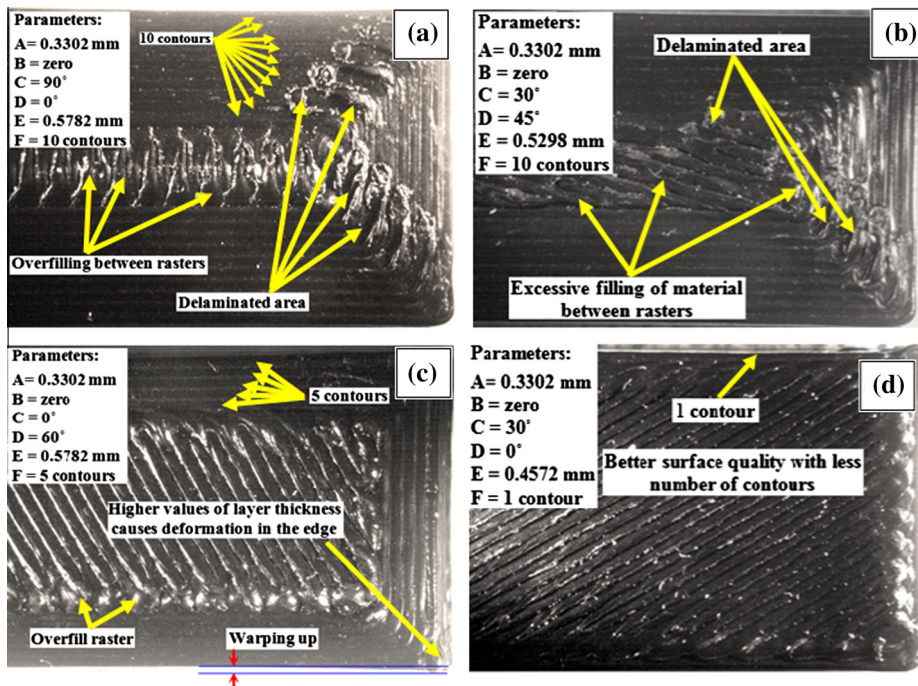


Fig. 12. Microscopic images revealing the effect of layer thickness and number of contours on percentage change in thickness for (a) sample No. 54, (b) sample No. 24, (c) sample No. 37 and (d) sample No. 21.

the machine will deposit 28 layers using slice thickness 0.127 mm and 11 layers using layer thickness 0.3302 mm. As a result, the actual thickness of the fabricated parts exceeds the theoretical thickness or the designed value specified by the CAD model. Therefore, it can be concluded that the greater the slicing thickness, the greater the deviation of the part thickness between the experimental and the designed value.

The interaction effects between layer thickness and build orientation on percentage change in thickness is shown in Fig. 11(b). From this figure, it is clear that layer thickness plays an important role in decreasing percentage change in thickness. It was observed that percentage change in thickness increases considerably with an increase in layer thickness and slightly with decrease in build orientation. This is so because a high value of layer thickness leads to increased heat generation, resulting in distortion and thermal expansion. The optimum value of percentage change in thickness (2.8672%) can be obtained when the lower value of layer thickness (0.1616 mm) and the highest value of build orientation (90°) were applied. Fig. 11(c and d) shows the 3D graph for interaction effects of layer thicknesses versus raster angle and layer thicknesses versus road width, respectively, on percentage change in thickness. It can be observed in Fig. 11(c) that, when layer thickness is set at the lowest level (0.127 mm) and raster angle is set at the highest level (90°), percentage change in thickness is at the minimum value, that is, 3.1713%, compared to other setting ranges. Conversely, when layer thickness is set at the highest level (0.3302 mm) and raster angle is set at the lowest level (0°), percentage change in thickness increases significantly

from 3.1713% to 9.2615%. Experimentally, it is observed that the increase of raster angle means shorter raster length, which also means small sharp angles. This helps to reduce the percentage change in thickness, in particular when using the highest level of build orientation (90°) because, under these conditions, the rasters are parallel to the specimen length. Fig. 11(d) shows the effect of layer thickness and road width on percentage change in thickness. The highest percentage dimensional error in thickness for this interaction effect was observed when the highest level of layer thickness and the center level of road width were applied. It can be seen in Fig. 11(d) that the minimum value (2.5241%) of percentage change in thickness can be obtained when layer thickness is set at the lowest level (0.127 mm) and road width is set at the highest level (0.5782 mm). Fig. 11(e) shows the response surface graph for the effect of layer thickness and number of contours on the percentage change in part thickness. It can be observed that layer thickness and number of contours have a significant effect on the percentage change in thickness. It can be seen from this figure that percentage change in thickness decreases significantly with decrease in layer thickness and number of contours. Percentage change in thickness exhibited a decrease to the minimum value (2.9806%) when the layer thickness of 0.1778 mm and 1 contour were applied.

To study the influence of number of contours on thickness, some samples with different number of contours, as shown in Fig. 12(a-d), were examined using a LEICA MEF4M light optical microscopy. Experimentally, it was noticed that, by using the highest value of layer thickness, and the lowest value of air gap with 10 contours, as shown

in Fig. 12(a and b), the surface of the parts will be prone to form wrinkles or ripples, resulting in excessive accumulation, deformation and overfilling in the top surface of the fabricated part and thus increase in the percentage change in thickness. However, from Fig. 12(c), it can be seen that by reducing the number of contours from 10 to 5, the surface of the part was improved and further improvement was observed with the use of only one contour, as shown in Fig. 12(d). Therefore, it can be concluded that the minimum number of contours is preferred for dimensional accuracy because it reduces the number of outer and inner loops, thus decreasing the accumulation of thermal expansion and residual stresses during deposition stage, and it thereby improves the accuracy of thickness of the part.

6. Multi-response simulation optimization using desirability function

FDM is a complex process that exhibits much difficulty in determining optimal parameters for the best quality of the part. Due to the presence of a large number of conflicting parameters and multi-factor interactions, the optimum setting of process parameters, which is needed for obtaining higher dimensional accuracy of fabricated part, is a challenging task. This can be obtained by applying the multi-criteria optimization technique. There are various methods for addressing the multi-criteria optimization problem. Previous work by Sood et al. [6] used gray relational grade (GRD) to combine the three responses into

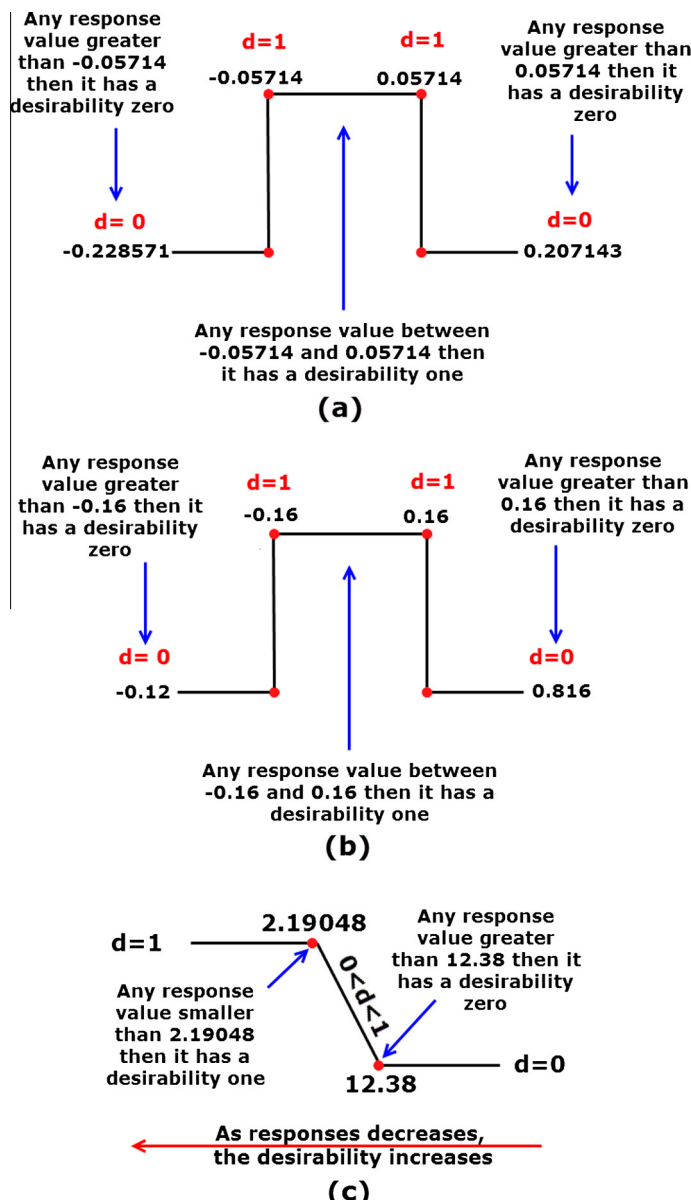


Fig. 13. Utility transfer function with goal is (a and b) in range and (c) minimize.

one response. However, GRD has some limitations and problems such as: (i) GRD varies with the change of relational coefficient of each individual comparison sequence; (ii) GRD suffers from Rank Reversal phenomenon, which is an instability phenomenon that occurs by the addition or deletion of one scheme or by change of local priorities; (iii) since FDM process has highly nonlinear characteristics, GRD does not detect the nonlinear relationships to estimate the true behavior in the response optimization in relation to process parameters. However, desirability function is the most widely used technique for such optimization. It provides better balance between the responses with little mathematical knowledge. It does not require any assumptions in the degree of estimated coefficients. Furthermore, desirability function is robust to potential dependency (linear and nonlinear relationships) between the process parameters and the responses.

In this study, Derringer's desirability function is used for optimization. In numerical optimization using desirability function, each response (y_i) must be transformed into an individual desirability (d_i), where $0 \leq d_i \leq 1$. In order to transform each response into an individual desirability, the fitness function 'goal is range', as expressed in Eq. (12), is used for percentage change in length and width to achieve accuracy within $\pm 0.05714\%$ (± 0.0199 mm) in length, and to achieve accuracy within $\pm 0.16\%$ (± 0.02 mm) in width. The fitness function 'goal is to minimize', as expressed in Eq. (13), is used for percentage change in thickness to minimize the error (less than

2.1905%). To determine the optimum process settings, a reduced gradient algorithm with sequential repetitions in multiple runs at different starting points that maximizes the desirability index was used. In order to determine the optimum process settings, specification of lower and upper limits for each factor and response was required. The Design Expert software was used to understand how different process conditions influence the responses. Design Expert software calculates the optimum process settings and draws the optimization plot. For example, if we want to minimize the response for part thickness (see Fig. 13 (c)), there is a need to specify the lower and upper limits (2.19048–12.38%) for the response value. The desirability for this response below 2.19048% is one and above the maximum value 12.38% is zero. The closer the response is to 2.19048%, the closer the desirability is to one. Fig. 13 shows the utility transfer function used to determine the individual desirability.

The final step is the transformation of an individual desirability (d_i) for all the responses into a single response using composite desirability, as expressed in Eq. (14) in order to determine the overall desirability of the multi-response optimization [22]. The parameter settings with maximum overall desirability are considered to be the optimal solution. For an ideal case, desirability is expected to be 1. However, if desirability is 0, it means that the response is outside the acceptable region [23]. The weights (r_i) can be assigned for each response to emphasize a target value or upper and lower values. The weights are used to

Table 8
Constraints of input parameters and responses.

Name	Goal	Lower limit	Upper limit	Lower weight	Upper weight	Importance
A: Layer thickness	Restricted to 0.127, 0.1778, 0.254, 0.3302	0.127	0.3302	1	1	3
B: Air gap	Is in range	0	0.5	1	1	3
C: Raster angle	Is in range	0	90	1	1	3
D: Build orientation	Is in range	0	90	1	1	3
E: Road width	Is in range	0.4572	0.5782	1	1	3
F: Number of contours	To be minimized and restricted to 1, 2, 3, 4, 5, 6, 7, 8, 9,10	1	10	1	1	3
% change in length	Is in range	–0.05714	0.05714	1	1	3
% change in width	Is in range	–0.1600	0.1600	1	1	3
% change in thickness	Minimize	2.1905	12.3800	1	1	3

Table 9
Optimum factor settings for high value of desirability.

Exp. no.	Optimum factor settings						Predicted responses (%)			Desirability index
	A	B	C	D	E	F	ΔL	ΔW	ΔT	
1	0.127	0.312	86.040	88.951	0.461	1	0.0520	–0.0360	2.0820	1.000
2	0.127	0.368	89.790	77.179	0.460	1	0.0560	0.0180	2.1770	1.000
3	0.127	0.318	87.140	84.539	0.458	1	0.0500	–0.0230	2.1100	1.000
4	0.127	0.348	89.575	81.830	0.463	1	0.0550	–0.0010	2.1340	1.000
5	0.127	0.342	88.918	89.122	0.462	1	0.0560	–0.0270	1.9780	1.000
6	0.127	0.370	89.255	77.828	0.459	1	0.0570	0.0160	2.1560	1.000
7	0.127	0.321	88.940	89.923	0.477	1	0.0560	–0.0130	2.1730	1.000
8	0.127	0.298	89.900	85.963	0.462	1	0.0430	–0.0280	2.1760	1.000
9	0.127	0.304	82.653	89.832	0.459	1	0.0530	–0.0430	2.1090	1.000
10	0.127	0.323	86.369	83.446	0.458	1	0.0520	–0.0160	2.1410	1.000

fine-tune the way in which the optimization process searches for the best solutions. The importance of each goal can be added to the responses; for example, one response is considered to be the most important in relation to the other responses. In most cases, there are many responses and the desirability of the outcome involves some or all of these responses [23]. For example, there are situations where the aim is to minimize one response and maximize another, while keeping the third response between the acceptable ranges or close to a certain target value.

$$d = \begin{cases} 1, & L < y \leq U \\ 0, & \text{Otherwise} \end{cases} \quad (12)$$

$$d = \begin{cases} 1 & y < T \\ \left(\frac{U-y}{U-T}\right)^r & T \leq y \leq U \\ 0 & y > U \end{cases} \quad (13)$$

where L and U are the lower and upper limits, T is the target, and r is the desirability weight.

$$D = (d_1 \times d_2 \times d_3 \dots \times d_n)^{\frac{1}{n}} = \left(\prod_{i=1}^n d_i \right)^{\frac{1}{n}} \quad (14)$$

where D is the composite desirability, n is the number of responses and $d_1, d_2, d_3 \dots d_n$ are individual desirability for a single response.

In this study, there are three optimization objectives (minimize, within range and constrained factors to be in specific levels). Furthermore, in previous section, it is clear that percentage change in length was improved with decrease in build orientation from 90° to 0° while percentage change in width and thickness were improved significantly with an increased in build orientation from 0° to 90° . Therefore, there are some conflicting objectives because of the different requirements of each of the responses. This is obtained by applying the multi-objective optimization technique. There are some physical restrictions imposed on the factor settings, which affect the selection of the optimal process settings and should be taken into account. The first practical constraint is that FDM Fortus 400 machine used in this study has only four specific values of layer thickness which are 0.1270, 0.1778, 0.2540 and 0.3302 mm because they are controlled by the tip size. The second practical constraint is that the levels of factor 'number of contours' are 1, 2, 3, 4 ... 10 and the FDM Fortus 400 machine will not allow to use any other fractional values, for example 1.5 or 6.5. Therefore, in optimization step, the constraints imposed on layer thickness and numbers of contours are considered in this study in order for the optimum parameter settings to be feasible and possible in practical applications. These constraints are shown in Table 8. From the 3D response surface plots discussed in the previous section, it is clear that the high value of number of contours is not preferred. Thus, minimizing the number of contours is considered to be the optimal value to achieve better accuracy and thus desirability function 'minimum-the-better' is selected for this factor. In the present study, Design Expert software has been used to optimize the output responses. From

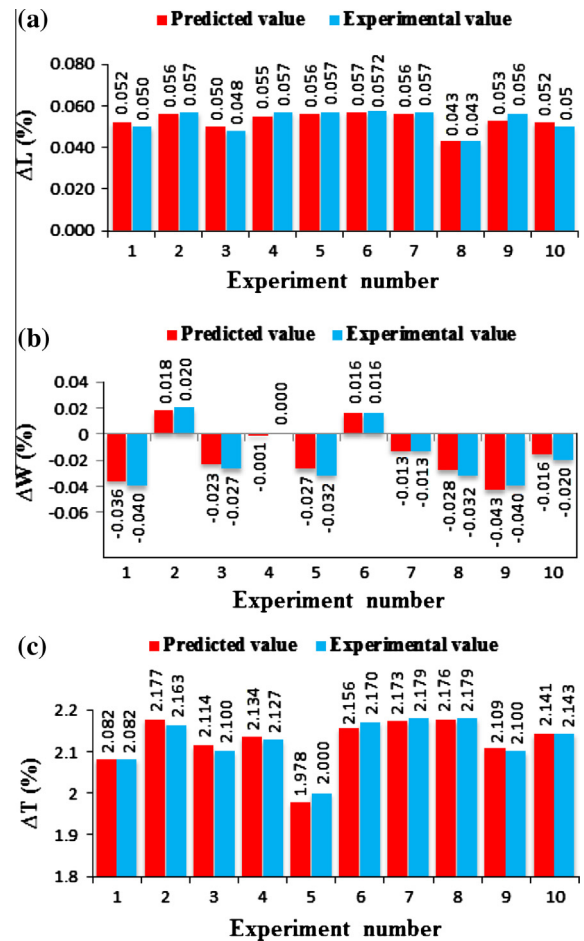


Fig. 14. Illustrative comparison between predicted results and experimental results for: (a) percentage change in length, (b) percentage change in width, and (c) percentage change in thickness.

the above settings, the optimal solutions were generated by the software. The percentage changes in length, width, and thickness were predicted according to the multi-objective optimization via desirability function, and the results are presented in Table 9. The maximum desirability is found to be 1 for 10 optimum solutions. This is revealing that the mathematical models developed in this study are highly reliable, which can be used in understanding adequately how various parameters involved will determine dimensional accuracy.

6.1. Confirmation experiments

The purpose of confirmation experiment is to verify the conclusions drawn from the experiment. From Table 9, it can be concluded that there was a set of 10 optimum settings producing a high value of desirability ($D = 1$). Therefore, 10 additional specimens were produced for confirmation experiment to validate the optimum parameter settings. Fig. 14(a–c) shows the comparison between predicted and experimental results for 10 optimum set-

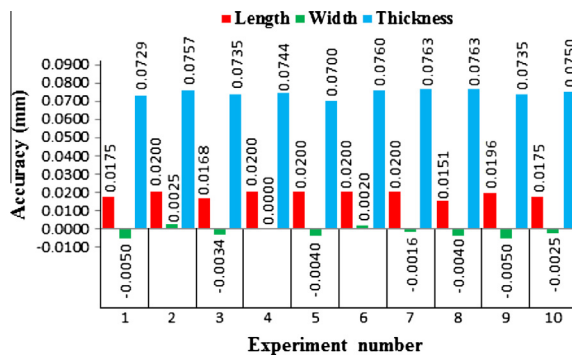


Fig. 15. Illustrative comparison between ten optimum settings in terms of obtained accuracy form experimental results for length, width, and thickness.

tings for the percentage changes in length, width, and thickness respectively. From Fig. 14(a–c), it can be noticed that the proposed method in this paper is better than other methods with respect to the better accuracy (quality of solutions) and the speed of computation. Simulations have shown that the proposed method has excellent performance, as the predicted values are very close to the experimental values with very little deviation. Furthermore, Fig. 15 shows the obtained accuracy from the real experiments using 10 optimum solutions. It can be observed from Fig. 15 that all 10 optimum settings achieved accuracy within the acceptable ranges. However, the best optimum setting for a global solution in terms of minimum deviations in length, width and thickness was obtained with optimum setting number 5 ($A = 0.127 \text{ mm}$, $B = 0.342 \text{ mm}$, $C = 88.918^\circ$, $D = 89.122^\circ$, $E = 0.462 \text{ mm}$ and

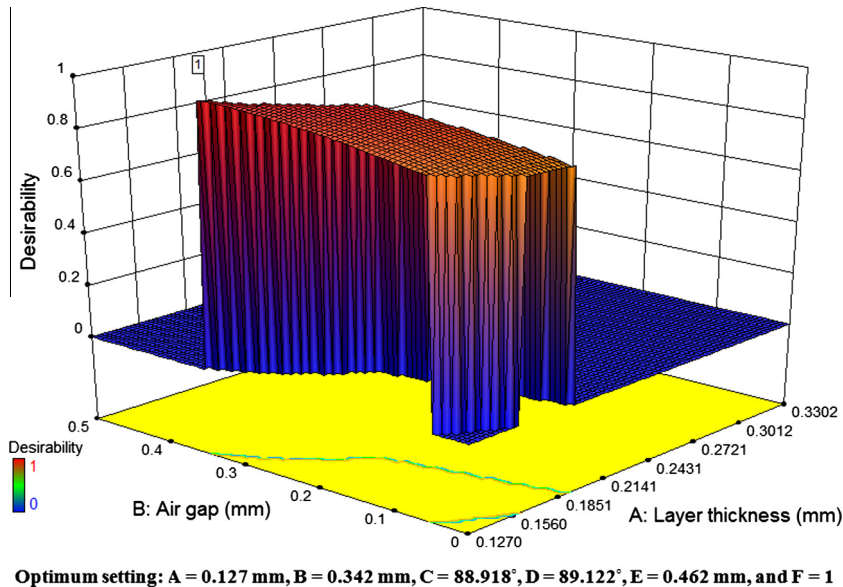


Fig. 16. Response surface plot of composite desirability for the best solution.

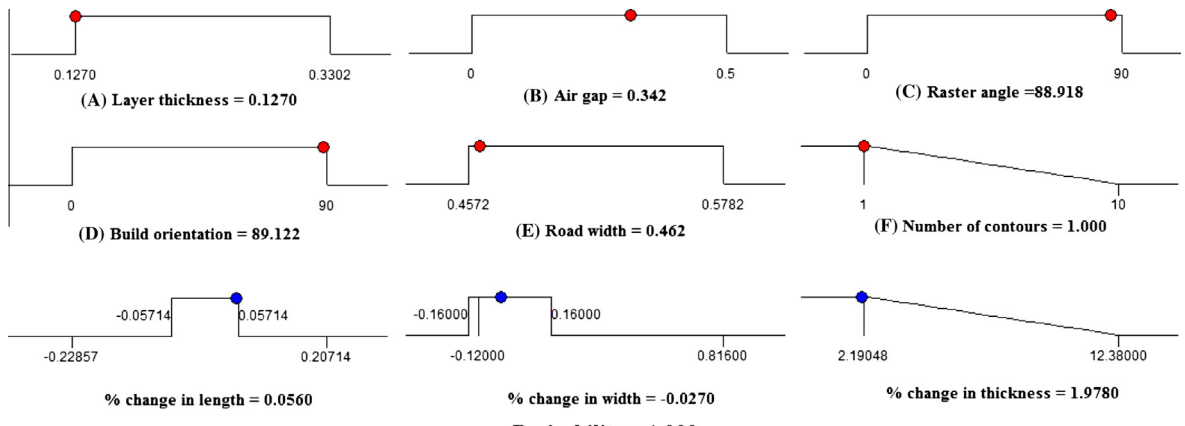


Fig. 17. Ramp function plot for results of overall desirability functions for optimal solution number 5 (best parameter settings for parameters), as derived from the mathematical models.

$F = 1$). The response surface plot of composite desirability for this optimum condition is shown in Fig. 16. This optimum setting achieved the global solution with accuracy (deviation) of +0.02 mm in length, accuracy of +0.004 mm in width, and accuracy of +0.007 in thickness. Fig. 17 is a ramp function plot showing optimal solution number 5 (best settings for parameters), as derived from the proposed method and mathematical models. It can be concluded that the proposed method is accurate, has high reliability and could be useful for engineers in estimating influence of wide range of process parameters. Clearly, this confirms excellent achievements of the experimental conclusions.

7. Conclusions

This study has described a methodology for an effective FDM process parameter optimization using I-optimal design. The study presented the successful application of I-optimal design in FDM process parameter optimization. The proposed method can effectively solve FDM part quality problems involving large number of parameters and levels that cannot be solved by traditional experiment design when many physical constraints and restrictions imposed on the experimental variables are included. In this study, the mathematical models were developed to describe the relationship between input parameters and dimensional accuracy. The following conclusions are drawn based on the results obtained from this study.

1. Results from statistical analysis have proved that the developed regression models can describe the relationship between input parameters and dimensional accuracy with a 95% confidence interval.
2. The parameters (layer thickness, air gap, build orientation, road width, and number of contours) show a significant effect on percentage change in length. A gradual increase in percentage change in length has been observed with increase in layer thickness (0.127–0.3302 mm), air gap (0–0.5 mm), build orientation (0°–90°), road width (0.4572–0.5782 mm) and number of contours (1–10). However, percentage change in length was reduced with increase in raster angle from 0° to 90°.
3. In the case of percentage change in width, the same trend, which is similar to percentage change in length, was presented. It was observed that the percentage change in width of the part decreases linearly with decrease in layer thickness, air gap, road width, and number of contours. However, it was improved significantly with an increased in build orientation and raster angle from 0° to 90°.
4. With an increase in layer thickness and number of contours from low to high level, percentage change in thickness also increases. However, the latter decreases with the increase in air gap, raster angle, build orientation, and road width, from low level toward high level.
5. Verification of the experiments shows that the predicted results are in very good agreement with experimental results. The results show that all 10 optimal

solutions give an acceptable accuracy in industrial applications. This assists additive manufacturing users in the appropriate selection of the optimal settings according to the desired accuracy.

6. Results obtained from the verification of experiments show that accuracy of +0.02 mm in length, +0.004 mm in width and +0.007 in thickness were obtained using developed models.
7. The experimental results also show that the best parameter settings (best solution) that can achieve better accuracy for all responses are: layer thickness of 0.127 mm; air gap of 0.342 mm; raster angle of 88.918°; build orientation of 89.122° road width of 0.462 mm, and 1 contour.

The work presented in this paper as a whole has confirmed that the proposed method was an adequate and efficient technique for FDM process parameter optimization. This method can be used in guiding the new applications of computer generated optimal design in optimization of process parameters for part quality in other additive manufacturing processes involving a wide range of process parameters.

References

- [1] S.H. Masood, Advances in fused deposition modeling, in: S. Hashmi (Ed.), *Comprehensive Materials Processing*, Science Direct Elsevier, 2014, pp. 69–88.
- [2] C.C. Kai, L.K. Fai, L. Chu-Sing, *Rapid Prototyping: Principles and Applications in Manufacturing*, World Scientific Publishing Co., Inc, 2003.
- [3] O.A. Mohamed, S.H. Masood, J.L. Bhowmik, Optimization of fused deposition modeling process parameters: a review of current research and future prospects, *Adv. Manuf.* (2015) 1–12.
- [4] C.K. Chua, K.F. Leong, C.S. Lim, *Rapid Prototyping: Principles and Applications*, World Scientific, 2010.
- [5] K. Cooper, *Rapid Prototyping Technology: Selection and Application*, CRC Press, 2001.
- [6] A.K. Sood, R. Ohdar, S. Mahapatra, Improving dimensional accuracy of fused deposition modelling processed part using grey Taguchi method, *Mater. Des.* 30 (2009) 4243–4252.
- [7] T. Nancharaiah, D.R. Raju, V.R. Raju, An experimental investigation on surface quality and dimensional accuracy of FDM components, *Int. J. Emerg. Technol.* 1 (2010) 106–111.
- [8] J.W. Zhang, A.H. Peng, Process-parameter optimization for fused deposition modeling based on Taguchi method, *Adv. Mater. Res.* 538 (2012) 444–447.
- [9] R.K. Sahu, S. Mahapatra, A.K. Sood, A study on dimensional accuracy of fused deposition modeling (FDM) processed parts using fuzzy logic, *J. Manuf. Sci. Prod.* 13 (2013) 183–197.
- [10] D.C. Montgomery, *Design and Analysis of Experiments*, John Wiley & Sons, 2008.
- [11] *ASTM D5418-07*, Standard Test Method for Plastics: Dynamic Mechanical Properties. Flexure (Dual Cantilever Beam), ASTM International, West Conshohocken, 2007.
- [12] *ASTM D7028-07e1*, Standard Test Method for Glass Transition Temperature (DMA Tg) of Polymer Matrix Composites by Dynamic Mechanical Analysis (DMA), ASTM International, West Conshohocken, 2007.
- [13] DMA2980, *Dynamic Mechanical Analysis. Operator's Manual*, TA Instrument, New Castle, 2002.
- [14] Stratasys, *Fortus Best Practice: Advanced Z calibration*, USA, 2014.
- [15] R.H. Myers, D.C. Montgomery, C.M. Anderson-Cook, *Response Surface Methodology: Process and Product Optimization Using Designed Experiments*, John Wiley & Sons, 2009.
- [16] W. Ahmed, M.J. Jackson, *Emerging Nanotechnologies for Manufacturing*, William Andrew, 2009.
- [17] S. Coleman, T. Greenfield, D. Stewardson, D.C. Montgomery, *Statistical Practice in Business and Industry*, John Wiley & Sons, 2008.

- [18] D.C. Montgomery, *Introduction to Statistical Quality Control*, John Wiley & Sons, 2007.
- [19] J.A. Cornell, *A Primer on Experiments With Mixtures*, John Wiley & Sons, 2011.
- [20] M.J. Anderson, P.J. Whitcomb, *RSM Simplified: Optimizing Processes Using Response Surface Methods for Design of Experiments*, Productivity Press, 2005.
- [21] T.-M. Wang, J.-T. Xi, Y. Jin, A model research for prototype warp deformation in the FDM process, *Int. J. Adv. Manuf. Technol.* 33 (2007) 1087–1096.
- [22] B. Dodson, P. Hammett, R. Klerkx, *Probabilistic Design for Optimization and Robustness for Engineers*, John Wiley & Sons, 2014.
- [23] G. Vining, *Statistical Process Monitoring and Optimization*, CRC Press, 1999.